ÉCOLE POLYTECHNIQUE FÉDÉRALE DE LAUSANNE
MATHICSE
Institute of Mathematics
School of Basic Sciences

MATHICSE Technical Report
Nr. 03.2017
February 2017

Dual dynamically orthogonal approximation of incompressible Navier Stokes equations with random boundary conditions

Eleonora Musharbash, Fabio Nobile

Address: EPFL - SB – MATHEMATICS INSTITUTE – Mathicse
(Bâtiment MA) Station 8 - CH-1015 - Lausanne - Switzerland

Dual Dynamically Orthogonal approximation of incompressible Navier Stokes equations with random boundary conditions

E. Musharbash[†] F. Nobile[†]

February 2, 2017

Abstract

In this paper we propose a method for the strong imposition of random Dirichlet boundary conditions in the Dynamical Low Rank (DLR) approximation of parabolic PDEs and, in particular, incompressible Navier Stokes equations. We show that the DLR variational principle can be set in the constrained manifold of all S rank random fields with a prescribed value on the boundary, expressed in low rank format, with rank smaller then S. We characterize the tangent space to the constrained manifold by means of a Dual Dynamically Orthogonal (Dual DO) formulation, in which the stochastic modes are kept orthonormal and the deterministic modes satisfy suitable boundary conditions, consistent with the original problem. The Dual DO formulation is also convenient to include the incompressibility constraint, when dealing with incompressible Navier Stokes equations. We show the performance of the proposed Dual DO approximation on two numerical test cases: the classical benchmark of a laminar flow around a cylinder with random inflow velocity, and a biomedical application for simulating blood flow in realistic carotid artery reconstructed from MRI data with random inflow conditions coming from Doppler measurements.

Introduction

Uncertainty quantification received a lot of attention in the last decades and is nowadays an active research field [22,24,40,41,45]. Mathematical models and numerical methods for efficient propagation of uncertainties are more and more needed in many application areas, from aerospace and mechanical engineering to life and geosciences. Numerical techniques for uncertainty propagation typically require a lot of problem solves for many values of the uncertain/random parameters and this may result in an unaffordable computational cost for complex applications, mostly if the phenomenon under study is time dependent. In this context, the use of reduced order models is very appealing as they reduce dramatically the computational cost of each solve, provided they guarantee a certain accuracy level. Many techniques have been developed, specially in the deterministic parametric framework, starting from the "classical" Proper Orthogonal Decomposition (POD) [5,8] and the Reduced Basis (RB) method [15,35]. All these techniques are based on the assumption that in many situations the solution manifold can be well approximated by a small number of dominant modes extracted from the covariance matrix of several snapshots precomputed in the offline stage, for different values of the parameters and different time instants. By performing a Galerkin projection into the subspace spanned by the dominant modes the size of the original problem is drastically reduced and the online stage simply consists in low-cost reduced-order simulations for new instances of the input. The drawback of this approach is that the solution manifold at time t, i.e. the collection $\mathcal{U}(t) = \{u(t,\omega), \omega \in \Omega\}$ of all solutions at time t for all

[†]Mathematics Institute, CSQI, École Polytechnique Fédérale de Lausanne, Switzerland

parameters $\omega \in \Omega$, may change significantly during the time evolution, which implies that the (fixed in time) reduced basis has to be sufficiently rich to be able to approximate $\mathcal{U}(t)$ at all time. This may lead to a fairly large reduced model thus compromising its efficiency.

An alternative approach that has been proposed in literature consists in expanding the solution on a fixed basis in the probability space by assuming that the randomness can be accurately parametrized in terms of a finite dimensional vector. For instance, in the Polynomial Chaos (PC) expansion, polynomial basis functions are chosen, which are orthonormal with respect of the underlying probability measure of the input random vector used to parametrize the stochastic space [22]. However, it has been reported in literature [43] that, for certain classes of problems, long time integration might need an increasing number of terms in the expansion to keep an acceptable accuracy level.

To overcome the limitations related to expansions of the solution on a fixed basis, either deterministic or stochastic, here we propose a dynamical low rank approximation. In the UQ context this method has been introduced in [38, 39] and is known under the name of Dynamically Orthogonal Field equations (DO). Equivalent formulations of the same approach can be found in [6,7] (Dynamically Bi-Orthogonal method or DyBO) and [9, 10] (Bi-Orthogonal method or BO). The DO is a reduced oder method in which both the spatial and random modes are computed on the fly and are free to evolve in time, thus adjusting at each time to the current structure of solution. The approximate solution is sought on the manifold $\mathcal{M}_S$ of S-rank functions $u_S(x,t,\omega) = \sum_{i=1}^{S} U_i(x,t)Y_i(t,\omega)$ with both $\{U_i\}$ and $\{Y_i\}$ linearly independent and is obtained by Galerkin projection of the governing equations onto the tangent space of $\mathcal{M}_S$ along the solution trajectory. As the manifold is parametrized in terms of dynamic constraints, one can derive evolution equations for both the deterministic modes U_i and the random modes Y_i, suitable for numerical computation. The same approach was independently proposed in literature in different fields. In the context of deterministic time-dependent Schrödinger equations its abstract formulation is known as Dirac-Frenkel time-dependent variational principle [25] and leads to the derivation of the so called multi-configuration time-dependent Hartree (MCTDH) method [2, 18, 30, 46]. In a finite dimensional setting the same is known as Dynamical Low Rank approximation [19, 21]. Extensions to tensor formats can be found in [11, 20, 27]. In [32] the link between the DLR, or MCTDH, and the DO method has been exploited to derive a quasi optimal error bound for the approximation of linear parabolic equations. More precisely the approximation error is bounded in terms of the best approximation error of the exact solution in $\mathcal{M}_S$, and holds in the largest time interval in which the best rank S approximation remains full rank and continuously differentiable in time.

In this paper we focus on the approximation of parabolic PDEs and, in particular, incompressible Navier-Stokes equations, with random Dirichlet boundary conditions. Our interest is motivated by the observation that, in fluid dynamics problems, small variations on inflow boundary conditions can have a strong impact on the dynamics of the flow. Applications can be found both in engineering and biomedical problems. A judicious approximation of the problem by low rank techniques necessarily has to address the issue concerning which boundary conditions should be satisfied by the approximate solution and if and how the randomness coming from the boundary should be compressed. This problem has not been investigated in depth in the literature so far, at least in the context of dynamically low rank approximation, and the answer is far from being straightforward. In fact it is not possible to say "a priori" which parameters have the strongest impact on the dynamics of the solution and at which time. Moreover no results can be derived by the comparison with the truncated Karhunen-Loève expansion which does not necessary approximate well the solution on the boundary. It is clear that the truncated Karhunen-Loève expansion, being the result of a (volumetric) L^2-projection at fixed time, is not able to quantify the discrepancy on the boundary and, least of all, evaluate its impact on the dynamics. We mention that in the first formulation of the DO method for random time dependent PDEs, as introduced in [38], the source of randomness includes boundary terms. The strategy proposed there consists in projecting the Dirichlet boundary conditions onto the subspace spanned by the stochastic modes at each time. However, we observe that this subspace evolves in time and is part of the solution of the approximate problem and not known "a priori". It is then not clear which boundary conditions are actually satisfied by the

approximate solution as times evolves and how the randomness arising from the boundary data is taken into consideration. An alternative approach, common in the reduced basis community [17,35], consists in computing explicitly a lift of the random boundary function, which needs to be written in separable form, and then solve for the homogeneous part of the solution (zero on the boundary). In such case, the deterministic modes always vanish on the boundary. However, on the one hand, the explicit construction of the lifting may be difficult and time consuming for time dependent random boundary conditions, and the quality of the approximation may be influenced by the choice of the lift. Theses issues are reflected in a similar way for the DO approximation and in particular the latter concerns the difficulty in evaluating the lost of information in deriving the reduced order system when the lift is projected in the tangent space.

In this work we investigate the possibility of strong imposition of the random boundary conditions in the dynamical low rank approximation. We require that the approximate solution satisfies the same boundary conditions as the eact solution, or a well controlled approximation of them. To do so we assume that the datum on the boundary is "almost low rank", which is not a too restrictive assumption in our context: since we are looking for an approximate solution u_S of rank S such that $u_S \approx u$, it is reasonable to ask that the boundary value $u_{|_{\partial D}} = g$ is properly approximated in separable form by $g_M = \sum_{i=1}^{M} Z_i(\omega) v_i(t,x)$ with $M \leq S$. In the context of dynamical low rank approximation, an approximation g_M of the boundary datum g in separable form with $M < S$ terms, will allow us to identify the proper boundary conditions to impose on each deterministic mode at each time for the solution $u_S = \sum_{i=1}^{S} U_i(x,t) Y_i(t,\omega)$. Indeed the reduced system for the evolution of the deterministic modes consists of S coupled PDEs of the same type as the original problem, which have to be completed with suitable boundary conditions. Our strategy consits in seeking for a dynamically low rank solution in the manifold $\mathcal{M}_S$ of rank S functions constrained to take the approximate value g_M on the boundary. We show, in particular, that, as long as the datum g_M has rank M, the constrained manifold is indeed a manifold and we provide a characterization of its tangent space. To derive a proper set of equations for the deterministic and stochastic modes, we propose a Dual-DO formulation, in which the stochastic modes are kept orthonormal, instead of the deterministic modes as in the original DO formulation of [38]. It turns out that such a formulation is very convenient for the "strong" imposition of random Dirichlet boundary conditions and results in a set of S coupled PDEs for the evolution of the deterministic modes (M of which with non homogeneous boundary conditions) coupled with $S - M$ ODEs for the evolution of the stochastic modes. Also when dealing with the incompressible Navier Stokes equations, the Dual-DO is also very convenient to include the incompressibility constraint.

The Dual DO method has been tested on two fluid dynamics problems. In the first one our goal is to test the performance of the Dual DO approximation in the challenging case in which the rank of the solution continues to increase in time. We consider the classical benchmark 2D problem of an incompressible viscous fluid flowing around a cylindrical obstacle in a channel at moderate Reynold numbers Re$\in [80, 120]$. The challenge of this test is due to the inflow velocity that depends on some random parameters. The patterns of the solutions correspond to flows with random vortex shedding frequency. Intuitively one can imagine the solution manifolds $\mathcal{U}(t)$ as the collection of infinitely many flow patterns which become more and more out of phase, one with respect to the others, as time evolves. The obtained numerical results show good performance of the method, at least in the initial phase, in approximating the whole solution manifold at each time instant with a relatively small number of time evolving modes. However, as one might expect, the performance deteriorates for larger times due to the "phase" issue. To alleviate the problem, we introduce a simple time rescaling based on an empirical linear relation between Reynolds number and shedding frequency considerably improves the performance of the method as it allows to "rephase" all solutions. In this setting we were able to simulate the transition phase and few shedding periods in the whole range Re$\in [80, 120]$ with good accuracy with $S = 4$ modes.

The second numerical problem addressed in this work aims at testing the possibility of applying the Dynamical Low Rank method for biomedical applications. Indeed in this field, numerical simulations of parameter dependent PDEs can be used as a virtual platform for the prediction of input/output response of biological

values, and the speed up of the computational time is a crucial issue. We consider the problem of simulating blood flow in a realistic carotid artery reconstructed from MRI data, where the inflow boundary conditions are taken as random due to the uncertainty and large errors in Doppler measurements of the inflow velocity profile [14,36]. The results highlight the remarkable potential of the Dual DO method for this type of problems. The paper is organized as follows: in Section 1 we introduce the problem setting and the notations used throughout, in Section 2 we recall the DO approach for a general parabolic problem with deterministic boundary conditions, in Section 3 we describe the Dual DO formulation for a second order elliptic operator with random Dirichlet boundary conditions and in Section 4 we applies the Dual DO to the Navier Stokes equations. Section 5 presents the two numerical tests mentioned above.

1 Problem setting and Notation

Let $D \subset \mathrm{R}^d$, $1 \leq d \leq 3$, be an open bounded domain and $(\Omega, \mathcal{A}, \mathcal{P})$ a complete probability space, where Ω is the set of outcomes, $\mathcal{A}$ a σ-algebra and $P : \mathcal{A} \to [0,1]$ a probability measure. We consider a general time dependent PDE of the type:

$$\dot{u}(x,t,\omega) = \mathcal{L}(u(x,t,\omega), x, t, \omega), \quad x \in D,\ t \in [0,T],\ \omega \in \Omega, \tag{1}$$

where $\mathcal{L}$ is a linear or non-linear differential operator, $x \in D$ is the spatial coordinate and t is the time variable in $[0,T]$. For the ease of notation in what follows we omit to write the explicit dependence of $\mathcal{L}$ on (x,t,ω) and use the shorthand notation $\mathcal{L}(u(x,t,\omega))$. The initial state of the system is described by

$$u(x,t=0,\omega) = u_0(x,\omega), \quad x \in D,\ \omega \in \Omega, \tag{2}$$

and equation (1) is complemented with suitable boundary conditions

$$\mathcal{B}(u(x,t,\omega),\omega) = g(x,t,\omega), \quad x \in \partial D,\ \omega \in \Omega,\ t \in [0,T].$$

Here $\omega \in \Omega$ represents a random elementary event which may affect the operator $\mathcal{L}$ (as e.g. a coefficient or a forcing term), the boundary conditions or the initial conditions. Specifically, in Section 4, we consider a second order deterministic elliptic operator $\mathcal{L}$ completed with random Dirichlet boundary conditions and in Section 4 we consider the Navier Stokes equations, with random viscosity and Dirichlet boundary conditions. We introduce here some notation that will be used throughout. Let $v : \Omega \to \mathbb{R}$ be an integrable random variable; we define the mean of v as:

$$\bar{v} = \mathbb{E}[v] = \int_\Omega v(\omega) d\mathcal{P}(\omega),$$

and the variance as:

$$\mathrm{Var}[v] = \mathbb{E}[(v-\bar{v})^2] = \int_\Omega (v(\omega)-\bar{v})^2 d\mathcal{P}(\omega).$$

We will use the shorthand notation: $v^* = v - \mathbb{E}[v]$, and $L^2_0(\Omega)$ will denote the set of all zero mean, square integrable random variables. Let now $v, u : D \times \Omega \to \mathbb{R}$ be x-indexed random fields. We denote the L^2 inner product in the physical space by:

$$\langle u(\cdot,\omega), v(\cdot,\omega)\rangle = \int_D u(x,\omega)v(x,\omega)dx.$$

We also recall that $L^2(D \times \Omega)$ denotes the space of all square integrable random fields, i.e.:

$$L^2(D \times \Omega) := \left\{ u : D \times \Omega \to \mathbb{R} \text{ s.t. } \int_D \mathbb{E}\big[(u(x,\cdot) - \bar{u}(x))^2\big] dx < \infty \right\}$$

Observe that $L^2(D \times \Omega)$ is isometrically isomorphic to $L^2(D) \otimes L^2(\Omega)$.
A vector-valued random field will be denoted by small bold letters $\mathbf{u} := (u_1, .., u_N)^T$ and is conventionally a column vector. The $L^2(D)$ and the $L^2(D \times \Omega)$ norms are respectively defined as:

$$\|\mathbf{u}(\cdot,\omega)\|^2_{[L^2(D)]^N} := \sum_{i=1}^N \|u_i(\cdot,\omega)\|^2_{L^2(D)} \text{ and } \|\mathbf{u}\|^2_{[L^2(D)]^N \otimes L^2(\Omega)} := \sum_{i=1}^N \|u_i\|^2_{L^2(D)\otimes L^2(\Omega)}.$$

In the following we will denote by $\|\cdot\|$ both the scalar and vector norm in $L^2(D \times \Omega)$. Capital bold letters will be instead used for denoting a vector of deterministic scalar (or vector-valued) functions $\mathbf{U} = (U_1, ..., U_S)$ (or $\mathbf{U} = (\mathbf{U}_1, ..., \mathbf{U}_S)$ in the case of vector valued functions) which will be written as row vector, and the notion $\ll \mathbf{U}, \mathbf{V} \gg$ denotes the $S \times S$ matrix with entries:

$$\ll \mathbf{U}, \mathbf{V} \gg_{ij} = \int_D V_i(x) U_j(x) dx$$

(or $\ll \mathbf{U}, \mathbf{V} \gg_{ij} = \int_D \mathbf{V}_i(x)^{\mathrm{T}} \mathbf{U}_j(x) dx$ if $\mathbf{U}_i, \mathbf{V}_j$ are vector functions).

Lastly, we recall the well known Karhunen-Loève expansion. Let $u \in L^2(D \times \Omega)$ be a square integrable random field, the covariance function $\mathrm{Cov}_u : \overline{D \times D} \to \mathbb{R}$ is defined as:

$$\mathrm{Cov}_u(x,y) = \mathbb{E}\left[u^*(x,\cdot) u^*(y,\cdot)\right], \quad x, y \in D.$$

and defines a trace class operator $T_u : L^2(D) \to L^2(D)$ as

$$T_u v(\cdot) = \int_D \mathrm{Cov}_u(x,\cdot) v(x) dx, \quad \forall v \in L^2(D); \tag{3}$$

Then, u can be written as:

$$u(x,\omega) = \bar{u}(x) + \sum_{i=1}^{\infty} \sqrt{\lambda_i} Z_i^{KL}(\omega) V_i^{KL}(x)$$

where:

- (λ_i, V_i^{KL}) are respectively the eigenvalues and the ($L^2(D)$-orthonormal) eigenfunctions of the covariance operator T_u,
- Z_i are mutually uncorrelated real-valued random variables given by:

$$Z_i^{KL}(\omega) := \frac{1}{\sqrt{\lambda_i}} \int_D u^*(x,\omega) V_i^{KL}(x) dx \qquad \forall i \in \mathbb{N}^+, \tag{4}$$

  with zero mean, $\mathbb{E}[Z_i^{KL}] = 0$, and unit variance, $\mathbb{E}[Z_i^{KL} Z_j^{KL}] = \delta_{ij}$.

Assuming that the eigenvalues are sorted in decreasing order, it is well known (see e.g. [13, 16, 23]) that the best L^2-approximation of u^* with S terms written in separable form is given by the truncated Karhunen-Loève

expansion:

$$u(x,\omega) \approx u_S^{KL}(x,\omega) := \bar{u}(x) + \sum_{i=1}^{S} \sqrt{\lambda_i} Z_i^{KL}(\omega) V_i^{KL}(x), \tag{5}$$

Assuming $\mathrm{Cov}_u \in C^0(\overline{D \times D})$ and D compact, by Mercer's theorem [37], it follows that

$$\lim_{S\to\infty} \sup_{x\in D} \mathbb{E}[(u(x,\cdot) - u_S^{KL}(x,\cdot))^2] = \lim_{S\to\infty} \sup_{x\in D} \sum_{i=S+1}^{\infty} \lambda_i (V_i^{KL}(x))^2 = 0.$$

All the previous definitions can be generalized to a time-varying random field $u(x,t,\omega)$ and in particular the Karhunen-Loève expansion can either be defined at each fixed $t \in [0,T]$:

$$u_S^{KL}(x,t,\omega) = \bar{u}(x,t) + \sum_{i=1}^{S} \sqrt{\lambda_i(t)} Z_i^{KL}(t,\omega) V_i^{KL}(x,t), \ \ \forall S \in \mathbb{N}^+ \tag{6}$$

with $\left\langle V_i^{KL}(\cdot,t), V_j^{KL}(\cdot,t) \right\rangle = \delta_{ij}$ for all $t \in [0,T]$, or as a global space-time approximation

$$\tilde{u}_S^{KL}(x,t,\omega) = \bar{u}(x,t) + \sum_{i=1}^{S} \sqrt{\lambda_i(t)} \tilde{Z}_i^{KL}(\omega) \tilde{V}_i^{KL}(x,t), \ \ \forall S \in \mathbb{N}^+,$$

provided $u \in L^2(D \times [0,T] \times \Omega)$. In what follows we refer always to (6) as the best S-terms approximation of a space-time random field.
Let us also define the Stiefel manifold $St(S,\mathcal{H})$, for a general Hilbert space $\mathcal{H}$, as the set of orthonormal frames of S vectors in $\mathcal{H}$, i.e.:

$$St(S,\mathcal{H}) = \left\{ \mathbf{V} = (V_1, ..., V_S) : V_i \in \mathcal{H} \text{ and } < V_i, V_j >_{\mathcal{H}} = \delta_{ij} \ \forall i,j = 1, ..., S \right\}$$

where $< \cdot, \cdot >_{\mathcal{H}}$ is the inner product in $\mathcal{H}$. We denote by $\mathcal{G}(S,\mathcal{H})$ the Grassmann manifold of dimension S that consists of all the $S-$dimensional linear subspaces of $\mathcal{H}$. Observe that the truncated Karhunen-Loève expansion can be characterized as:

$$u_S^{KL}(x,t,\omega) = \Pi_{\mathcal{V}_S^{KL}(t) \otimes \mathcal{Z}_S^{KL}(t)} \left[u_S(x,t,\omega) \right] \tag{7}$$

where Π is the $L^2(D \times \Omega)$ projector and $\mathcal{V}_S^{KL}(t) \in \mathcal{G}(S, L^2(D))$, $\mathcal{Z}_S^{KL}(t) \in \mathcal{G}(S, L^2(\Omega))$ coincide respectively to the span of the first S deterministic and stochastic modes: $(V_1^{KL}, ..., V_S^{KL}) \in St(S, L^2(D))$ and $(Z_1^{KL}, ..., Z_S^{KL}) \in St(S, L^2(\Omega))$, in the Karhunen-Loève expansion (6).
However we would like to emphasize that, in our context, the Karhunen-Loève decomposition (6) of the solution to problem (1), as well as the L^2-orthogonal projector $\Pi_{\mathcal{V}^{KL} \otimes \mathcal{Z}^{KL}}$ in (7), are not available in practice. In other words the optimality of the Karhunen-Loève approximation is suitable only for the purpose of analysis, since it provides a lower bound for the approximation error of low rank methods.

2 Dynamical Low rank methods

The Dynamical Low rank approach [19, 25] is a reduced order method according to which the solution of the governing equation is approximated in a low dimensional manifold of functions with fixed rank, written in

separable form. The peculiarity of this reduced basis approach relies on the fact that both the deterministic modes and the stochastic coefficients can evolve in time and are thus able to dynamically adapt to the features of the solution. The approximate solution is obtained by performing a Galerkin projection of the governing equations onto the (time-varying) tangent space to the approximation manifold along the solution trajectory. Let us assume that the solution $u(\cdot, t, \omega)$ to problem (1) is in a certain Hilbert space $\mathcal{H} \subset L^2(D)$ for (almost) all $t \in [0, T]$ and $\omega \in \Omega$ and that $\mathcal{L}(u) \in \mathcal{H}'$ for all $u \in \mathcal{H}$ and almost everywhere in $[0, T] \times \Omega$. Moreover let us define S *rank random field* any function $u_S \in \mathcal{H} \otimes L^2(\Omega)$ which can be expressed as a sum of S (and not less than S) linearly independent deterministic modes combined with S linearly independent stochastic modes.

Definition 2.1. *We define $\mathcal{M}_S \subset \mathcal{H} \otimes L^2(\Omega)$ the manifold of all the S rank random fields, i.e.:*

$$\mathcal{M}_S = \left\{ u_S \in \mathcal{H} \otimes L^2(\Omega) : u_S = \sum_{i=1}^{S} U_i Y_i \,|\quad \begin{array}{l} \textit{span}(U_1, ..., U_S) \in \mathcal{G}(S, \mathcal{H}), \\ \textit{span}(Y_1, ..., Y_S) \in \mathcal{G}(S, L^2(\Omega)) \end{array} \right\} \tag{8}$$

Observe that the definition of S rank random field can be characterized in several different ways. We recall in the following box few of the many possible representations that have been proposed and used in literature. For simplicity we describe the different options for time independent random fields.

Representations of S rank random field:

- *Double-Orthogonal decomposition* (used e.g. in [19, 21]), thereafter named DDO:

$$u_S(x, \omega) = \sum_{i=1}^{S} \sum_{j=1}^{S} \mathbf{A}_{ij} Z_i(\omega) V_j(x) = \mathbf{V} \mathbf{A} \mathbf{Z}^T \tag{9}$$

  where:
  - $\mathbf{A}_{ij} \in \mathbb{R}^{S \times S}$ is a full rank matrix,
  - $\mathbf{V}$ is a row vector of S $L^2(D)-$orthonormal deterministic functions,
  - $\mathbf{Z}$ is a row vector of S $L^2(\Omega)-$orthonormal random variables.

- *Decomposition with orthonormal deterministic modes* (used e.g. in [38, 39]), thereafter named DO:

$$u_S(x, \omega) = \sum_{i=1}^{S} \tilde{Y}_i(\omega) \tilde{U}_i(x) = \tilde{\mathbf{U}} \tilde{\mathbf{Y}}^T \tag{10}$$

  where:
  - $\tilde{\mathbf{U}} = \mathbf{V}$ is a row vector of $L^2(D)-$orthonormal deterministic functions,
  - $\tilde{\mathbf{Y}} = \mathbf{Z}\mathbf{A}^T$ is a row vector of S linearly independent random variables, hence with full rank covariance matrix $\mathbf{C} = \mathbb{E}[\tilde{\mathbf{Y}}^T \tilde{\mathbf{Y}}]$.

- *Decomposition with orthonormal stochastic modes* (see Section 3), thereafter named Dual DO:

$$u_S(x, \omega) = \sum_{i=1}^{S} Y_i(\omega) U_i(x) = \mathbf{U} \mathbf{Y}^T \tag{11}$$

  where:
  - $\mathbf{U} = \mathbf{V}\mathbf{A}$ is a row vector of S linearly independent deterministic functions. Namely, $\mathbf{M} \in \mathbb{R}^{S \times S}$, defined as $\mathbf{M}_{ij} = \langle U_j, U_i \rangle$, is a full rank matrix.
  - $\mathbf{Y} = \mathbf{Z}$ is a row vector of S $L^2(\Omega)-$orthonormal random variables.

In this paper we adopt the *decomposition with orthonormal stochastic modes* that turns out to be more suitable to approximate the incompressible Navier Stokes equations with random Dirichlet boundary conditions.
Observe, however, that none of the previous formats leads to a unique representation of u_S. Namely it is always possible to rewrite u_S in the same format but with a different set of bases. This implies that the Dynamical Low Rank solution (DLR solution), or generally any arbitrary continuously differentiable path $t \to u_S(t)$ from $[0,T]$ to $\mathcal{M}_S$, is not uniquely described in terms of time dependent bases, whatever the format in which it is represented is. However, the uniqueness of the representation is recovered by imposing dynamic constrains in the evolution of the bases. These constraints can be formally derived by exploiting the geometrical differential structure of the approximation manifold, see Section 3 and [1, 25, 29].

2.1 DLR Variational Principle

We introduced here the Dynamical Low Rank (DLR) approach for a general problem (1), all details concerning the boundary conditions conditions have been postponed to Section 3.2.
Consider problem (1): the solution u describes a path $t \to u(t)$ from $[0,T]$ in $\mathcal{H} \otimes L^2(\Omega)$. The idea behind the DLR approach is to approximate this curve $t \to u(t) \approx u_S(t)$ by dynamically constraining the time derivative $\dot{u}_S$ to be in the tangent space to the manifold $\mathcal{M}_S \subset \mathcal{H} \otimes L^2(\Omega)$ at $u_S(t)$ by Galerkin projection of the governing equation (1). Precisely, the DLR variational principle for problem (1) reads as follows:

Proposition 2.1. *At each $t \in [0,T]$, find $u_S(t) \in \mathcal{M}_S$ such that:*

$$\mathbb{E}\left[\langle \dot{u}_S(\cdot,t,\cdot) - \mathcal{L}(u_S(\cdot,t,\cdot)), v\rangle\right] = 0, \quad \forall v \in \mathcal{T}_{u_S(t)}\mathcal{M}_S \tag{12}$$

where $\mathcal{T}_{u_S(t)}\mathcal{M}_S$ is the tangent space to $\mathcal{M}_S$ at $u_S(t)$.

If $\mathcal{L}(u_S(\cdot,t,\cdot))$ is in the tangent space itself at $u_S(t)$ for any $u_S \in \mathcal{M}_S$, and at any time, and u_0 is a S rank function, then the DLR approximation recovers the exact solution. If u_0 is not S rank and the DLR method is initialized with its best S rank approximation, u_{0S}^{KL}, then the DLR solution coincides with the truncated Karhunen-Loève expansion (i.e. the best S rank approximation), under the assumption that the eigenvalues considered in the approximation of u_0 do not cross the ones that have been omitted at initial time [32].
Observe that the variational principle in (12) does not depend on the parametrization of the manifold $\mathcal{M}_S$, as long as the solution is full rank. Specifically, the tangent space $\mathcal{T}_{u_S(t)}\mathcal{M}_S$ is time dependent and depends only on $u_S(t)$ and not on its representation. The variational principle in (12) provides indeed an unified formulation for the DO method, as proposed by Sapsis [38], and similar approaches proposed in literature, including the DyBO method [6] and the DDO method [11]. We refer to [32] for further details.
In order to numerically compute the approximate solution one needs to uniquely characterize u_S in terms of deterministic and stochastic bases (modes). This is achieved by locally characterizing the manifold by means of a parametrization of the tangent space. This is detailed in the next section for the Dual DO formulation with orthonormal stochastic modes.

3 Dual DO formulation

We have seen that from the variational point of view, the DLR approximate solution $u_S \in \mathcal{M}_S$ is defined as a solution of the variational principle (12) at each time. However to numerically compute u_S, we need to parametrize the tangent space, hence the manifold, in terms of local charts, corresponding in our context to the deterministic and stochastic modes. Once a parametrization has been fixed, one can easily derive a set of equations that uniquely describe the dynamics of both the deterministic and stochastic modes. We emphasize

that problem (12) leads to different sets of equations depending on the parametrization of the tangent space and any of these parametrizations leads to a different reduced order system. Here we adopt the two fields formulation (11) in which we assume the stochastic modes to be orthonormal. We will refer to it as *Dual DO Formulation* (as opposed to (10) which keeps the deterministic modes orthonormal and was originally proposed in [38]). This representation turns out to be computationally more efficient and more suitable for dealing with random Dirichlet boundary conditions and solenoidal constraints. We define:

$$\mathcal{B}_{[\mathcal{H}]^S} = \{\mathbf{U} = (U_1, ..., U_S) : U_i \in \mathcal{H} \text{ with } \mathbf{M}_{ij} =< U_i, U_j > \text{ s.t. } \text{rank}(\mathbf{M}) = S\}$$

and the map:

$$\begin{array}{lll} \tilde{\pi}: & \left(\mathcal{B}_{[\mathcal{H}]^S}, St(S, L^2(\Omega))\right) & \to \mathcal{M}_S \subset \mathcal{H} \otimes L^2(\Omega) \\ & (\mathbf{U}, \mathbf{Y}) & \mapsto \tilde{\pi}(\mathbf{U}, \mathbf{Y}) = \sum_{i=1}^S U_i Y_i =: u_S \end{array} \tag{13}$$

The image of $\tilde{\pi}$ is the manifold of S rank random fields $\mathcal{M}_S$ defined in (8). Observe that:

- the DO variational principle (12) is defined in $\mathcal{M}_S$ while we want to write the DLR approximate solution in terms of $(\mathbf{U}, \mathbf{Y}) \in \mathcal{B}_{[\mathcal{H}]^S} \times St(S, L^2(\Omega))$;
- the map $\tilde{\pi}$ is not injective, indeed for any orthogonal matrix $\mathbf{Q} \in \mathbb{R}^{S \times S}$, $\tilde{\pi}(\mathbf{UQ}, \mathbf{Q}^T\mathbf{Y}) = \tilde{\pi}(\mathbf{U}, \mathbf{Y})$.

The uniqueness of the representation (13) can be recovered in terms of unique decomposition in tangent space by imposing the following Gauge constraint [12, 29]:

$$\mathbb{E}[\delta Y_i Y_j] = 0 \qquad \forall i, j = 1, ..., S, \tag{14}$$

which leads to the following parametrization of the tangent space at $u_S = \sum_{i=1}^S U_i Y_i$ as [19, 31]:

$$\begin{array}{lll} \mathcal{T}_{u_S}\mathcal{M}_S & = \Big\{ \dot{v} = \sum_{i=1}^S \left(\delta U_i Y_i + U_i \delta Y_i\right) & \in \mathcal{H} \otimes L^2(\Omega), \text{ with } \delta U_i \in \mathcal{H}, \\ & & \delta Y_i \in L^2(\Omega) \text{ s.t. } \mathbb{E}[\delta Y_i Y_j] = 0 \ \forall i, j = 1, ..., S \Big\}. \end{array} \tag{15}$$

Finally the variational problem (12) can be rewritten in terms of evolution equations for $(\mathbf{U}, \mathbf{Y})$.

Proposition 3.1. *Let $(\mathbf{U}(t), \mathbf{Y}(t)) \in \mathcal{B}_{[\mathcal{H}]^S} \times St(S, L^2(\Omega))$ be a solution of the following system:*

$$\frac{\partial U_i(x,t)}{\partial t} = \mathbb{E}\left[\mathcal{L}(u_S(x,t,\cdot))Y_i(t,\cdot)\right] \qquad i = 1, \cdots, S \tag{16}$$

$$\sum_{i=1}^S \mathbf{M}_{ji}(t) \frac{\partial Y_i(t,\omega)}{\partial t} = \Pi^{\perp}_{\mathcal{Y}} \left\langle \mathcal{L}(u_S(\cdot,t,\omega)), U_i(\cdot,t) \right\rangle \qquad j = 1, \cdots, S \tag{17}$$

then $u_S(t) = \tilde{\pi}(\mathbf{U}(t), \mathbf{Y}(t)) \in \mathcal{M}_S$ satisfies the DLR variational principle (12) at any $t \in [0, T]$.

Note the symmetry with the DO system proposed in [38].

3.1 Isolating the mean

In our context of partial differential equations with random parameters, since we are usually interested in computing the statistics of the solution, it may be worth approximating separately the mean of the solution. This is achieved by adopting a slightly different definition of S-rank random field and leads to an approximation closer to the Karhunen-Loève expansion of the solution (5) where the mean is treated separately in the

expansion. The idea of isolating the mean and the corresponding DO formulation was introduced in [38] and adopted in [39], [32], [6]. We detail here only the Dual DO formulation and re-define S rank random field as follows.

Definition 3.1. *We call S rank random field (with the isolating mean format) any function that can be exactly expressed as:*

$$\begin{array}{lll} u_S & = \bar{u}_S & +\sum_{i=1}^{S} U_i Y_i \\ & = U_0 Y_0 & +\sum_{i=1}^{S} U_i Y_i \quad = \mathbf{U}\mathbf{Y}^{\mathrm{T}} \end{array} \tag{18}$$

where:

- $\mathbf{Y}$ *is a row vector of $S+1$ $L^2(\Omega)$-orthonormal random variables such that $Y_0 = 1$ and $\mathbb{E}[Y_i] = 0$ for all $i = 1, ..., S$,*
- $U_1, ..., U_S$ *are linearly independent deterministic functions.*

One can think that the difference with respect to definition (11) consists in fixing the first random variable to be constant ($Y_0 = 1$), with the zero mean condition of the remaining random variables coming simply from the orthonormality of the random modes. However, observe that (18) is not necessarily a $S+1$ rank function since $\bar{u}_S$ is not assumed to be linearly independent of $U_1, ..., U_S$, or more precisely the subspace spanned by $\mathbf{U}$ does not have necessarily dimension $S+1$ (*at most* dimension $S+1$ and at least S). According to the new definition of S rank random field given in (18) the Dual DO system derived in (16)-(17) becomes:

$$\dot{U}_0(x,t) = \mathbb{E}\left[\mathcal{L}(\tilde{u}_S(x,t,\cdot))\right] \tag{19}$$

$$\dot{U}_i(x,t) = \mathbb{E}\left[\mathcal{L}(\tilde{u}_S(x,t,\cdot))Y_i(t,\cdot)\right] \qquad i = 1, \cdots, S \tag{20}$$

$$\sum_{j=1}^{S} \mathbf{M}_{ji}(t)\dot{Y}_j(x,t) = \Pi_{\mathcal{Y}}^{\perp} \left\langle \mathcal{L}^*(\tilde{u}_S(\cdot,t,\omega),\omega), U_i(\cdot,t)\right\rangle \qquad i = 1, \cdots, S \tag{21}$$

$$= \Pi_{\tilde{\mathcal{Y}}}^{\perp} \left\langle \mathcal{L}(\tilde{u}_S(\cdot,t,\omega),\omega), U_i(\cdot,t)\right\rangle \qquad i = 1, \cdots, S \tag{22}$$

where $\mathcal{Y} = span(Y_1, ..., Y_S)$, $\mathcal{L}^*(\tilde{u}_S(x,t,\omega),\omega) := \mathcal{L}(\tilde{u}_S(x,t,\omega),\omega) - \mathbb{E}[\mathcal{L}(\tilde{u}_S(x,t,\cdot))]$, $\tilde{\mathcal{Y}} = span(Y_0, ..., Y_S)$ and $\mathbf{M}_{ij} = \langle U_j, U_i\rangle$, $i, j = 1, ..., S$.

Remark 1. *Observe that definition (18) does not guarantee the optimality in the manifold of function with rank $S+1$. This is due to the fact that we do not assume U_0 linearly independent of $U_1, ..., U_S$ and so (18) may have a deficient rank. To clarify this point, just consider the function $u(x,\omega) = x + \alpha(\omega)x$, with $\mathbb{E}[\alpha] \neq -1$. This is clearly a 1-rank function, but representation (18) would require 2 modes.*

The previous remark may appear quite obvious when we only want to isolate the mean, but it turns out to be a crucial point when the number of constraints is larger. In the following we investigate the latter situation. For this purpose, the main questions that we need to address are: how to define the low rank manifold with constraints and which is the best approximation in this manifold.

3.2 Dual DO under boundary constraints

We now explicitly assume that $\mathcal{L}$ in (1) is a second order elliptic operator of the form $\mathcal{L}(u) = -div(A(x,\omega)\nabla u) - b(x,\omega)\cdot\nabla u + c(x,\omega)u \oplus f(x,t,\omega)$ where $A_{ij}(x,\omega), b_i(x,\omega), c(x,\omega)$, $i,j = 1, ..., d$, are bounded random variables in the open bounded Lipschitz domain $D \subset \mathbb{R}^d$ and under the assumptions that $A(x,\omega)$ is uniformly

coercive almost surely and $f \in L^2([0,T], L^2(D \times \Omega))$. The problem is set in $H^1(D) \otimes L^2(\Omega)$ and completed with Dirichlet boundary conditions $u_{|\partial D} = g$. If the boundary condition is deterministic it is reasonable to adopt formulation (18) in which the first deterministic mode, that approximates the mean, is required to fulfill the constraint on the boundary, while all other modes satisfy homogeneous conditions:

- $U_0(x,t) = g(x,t)$ for $x \in \partial D$,
- $U_i(x,t) = 0$ for $x \in \partial D$ and for all $i = 1, ..., S$.

This is consistent with the Karhunen-Loève decomposition given in (5), for which we have:

$$\begin{aligned} \lambda_i V_i^{KL}(y)_{|\partial D} &= \left[\int_D \mathrm{Cov}_u(x,y) V_i^{KL}(x) dx\right]_{|_{y \in \partial D}} \\ &= \int_D \mathbb{E}\left[u^*(x,\cdot) u^*(y,\cdot)_{|_{y \in \partial D}}\right] V_i^{KL}(x) dx = 0 \qquad \forall i \in \mathbb{N}^+ \end{aligned} \tag{23}$$

since $\bar{u}_{|\partial D} = \mathbb{E}[u]_{|\partial D} = g$ and $u^*_{|\partial D} = u_{|\partial D} - \bar{u}_{|\partial D} = 0$. The case in which the boundary data are random is more cumbersome. The first question to be addressed is which boundary conditions should be satisfied by a general low rank approximate solution. One can easily verify that the truncated Karhunen-Loève expansion does not necessarily satisfy the same boundary conditions satisfied by the exact solution. Consider for example the following toy problem in D $\equiv (0, 2\pi)$:

$$\begin{cases} \dot{u}(x,t,\omega) - \Delta u(x,t,\omega) = 0 \\ u(0,t,\omega) = u(2\pi,t,\omega) = \alpha(\omega) e^{-t} \\ u(x,0,\omega) = \alpha(\omega)\cos(x) + \beta(\omega)\sin(x) \end{cases} \tag{24}$$

where α, β are two uncorrelated zero mean random variables such that $\mathbb{E}[\alpha^2] < \mathbb{E}[\beta^2]$. The exact solution is $u(x,t,\omega) = e^{-t}(\alpha(\omega)cos(x) + \beta(\omega)sin(x))$. It is clear that the Karhunen-Loève approximate solution of rank 1 is $u_1^{KL}(x,t,\omega) = \beta(\omega) e^{-t}\sin(x)$ and $u^{KL}_{1|\partial D} \neq u_{|\partial D}$. Generally the values of the truncated Karhunen-Loève expansion on the boundary are unknown. Secondly, in the context of Dynamical Low Rank approximation, we need to specify the boundary conditions to impose on each deterministic mode $U_1, ..., U_S$. We remind that the Dual DO reduced system consists of dynamic differential equations for all the factors in (11). In particular, in the equations (16)-(17), boundary conditions for each deterministic mode U_i are needed to have a well posed problem.

Dual DO under random boundary constraints

Our strategy consists in enforcing that the low rank approximation satisfies the same boundary conditions as those of the exact solution. This is motivated by the fact that we can not say "a priori" which parameters have the strongest impact on the dynamics and at which time the dynamic of the solution is influenced by the uncertain parameters in the boundary data. It may therefore be important to impose these constraints as accurately as possible. To do so we assume that the datum on the boundary is "almost low rank", which is not a too restrictive assumption in our context: since we are looking for an approximate solution $u_S \approx u$ is reasonable to ask that $u_{|\partial D}$ is properly approximated by a function of rank at most S. We start considering Dirichlet boundary conditions that do not depend on time.

Assumption 1. *The boundary function g can be properly approximated on the manifold of M-rank functions for some $M \leq S$:*

$$u(x,t,\omega) = g(x,\omega) \approx g_M(x,\omega) = \sum_{i=1}^{M} v_i(x) Z_i(\omega) \quad \forall x \in \partial D, \ \ \textit{a.s.} \tag{25}$$

with:

- $\mathbb{E}[Z_i Z_j] = \delta_{ij}$,
- $v_1, ..., v_M$ *linearly independent.*

We denote by R the difference $S - M$ and by $\mathcal{Z}$ the subspace spanned by $\{Z_1, ..., Z_M\}$. Then in the DO formulation (12), we impose strongly condition (25). Precisely we ask:

$$u_S(x, t, \omega) = g_M(x, \omega) \quad \forall x \in \partial D, \text{ a.s.} \tag{26}$$

For the sake of clarity, we start considering a general Dual DO representation, as defined in (11). The similar formulation with the isolation of the mean is discussed in Remark 2.

Definition 3.2. *A S rank random field under constraint (26) is a S rank function that satisfies the boundary condition in (25) and can be written as:*

$$u_S^{g_M}(x, \omega) = \sum_{i=1}^{S} U_i(x) Y_i(\omega) = \mathbf{U}\mathbf{Y}^T \tag{27}$$

with:

- $u_{S|_{\partial D}} = g_M$ *a. s.,*
- $U_1, ..., U_S$ *linearly independent deterministic functions.*
- $Y_1, ..., Y_S$ *uncorrelated random variables.*

We denote by $\mathcal{M}_S^{g_M}$ the set of all the S rank random fields under constraint (26).

For the sake of notation, we omit the superscript in $u_S^{g_M}$ in the following. However observe that definition (27) strongly depends on the boundary conditions. Our first aim is to show that $\mathcal{M}_S^{g_M}$ is indeed a manifold. and precisely we aim to show that $\mathcal{M}_S^{g_M}$ is the *manifold* of all random fields of rank S that satisfy the same boundary condition as the solution, up to the approximation in (25). We now claim that any function in $\mathcal{M}_S^{g_M}$ can be written in terms of the random modes $Z_1, ..., Z_M$ in (25) and $R = S - M$ "free" random variables, in the orthogonal complement of $\mathcal{Z}$.

Lemma 3.1. *Let $\mathcal{M}_{R,M}$ denote the manifold of all the functions $u_{R,M}$ written as:*

$$u_{R,M}(x, \omega) = \sum_{i=1}^{R} U_i(x) Y_i(\omega) + \sum_{i=1}^{M} V_i(x) Z_i(\omega) \tag{28}$$

where we assume:

- $R + M = S$,
- $u_{R,M}(x, \omega) = g_M(x, \omega) = \sum_{i=1}^{M} v_i(x) Z_i(\omega)$ *for $x \in \partial D$ a.s.,*
- *all the random variables are mutually $L^2(\Omega)$-orthonormal:*
  - $\mathbb{E}[Z_i Z_j] = \delta_{ij}$ *for all $i, j = 1, ..., M$;*
  - $\mathbb{E}[Y_i Y_j] = \delta_{ij}$ *for all $i, j = 1, ..., R$;*

– $\mathbb{E}[Z_i Y_j] = 0$ *for all* $i = 1, ..., M$ *and for all* $j = 1, ..., R$.

- $U_1, ..., U_R$ *are linearly independent.*

Then, the set $\mathcal{M}_S^{g_M}$ *coincides with* $\mathcal{M}_{R,M}$*, hence it is a manifold.*

To prove this lemma we need a preliminary result:

Lemma 3.2. *Given a random field* $u_{R,M} \in \mathcal{M}_{R,M}$ *defined as in (28), it holds:*

- $V_{i|_{\partial D}} = v_i$ *a.s. for all* $i = 1, ..., M$*;*
- $U_{i|_{\partial D}} = 0$ *a.s. for all* $i = 1, ..., R$*;*

and in particular $\{U_1, ..., U_R, V_1, ..., V_M\}$ *are linearly independent.*

Proof. To verify the values of U_i and V_i on the boundary is enough to observe that:

$$\begin{aligned} V_{i|_{\partial D}} &= \mathbb{E}[u_{R,M|_{\partial D}} Z_i] = \mathbb{E}[g_M Z_i] = \textstyle\sum_{j=1}^{M} v_j \mathbb{E}[Z_j Z_i] = v_i \\ U_{i|_{\partial D}} &= \mathbb{E}[u_{R,M|_{\partial D}} Y_i] = \mathbb{E}[g_M Y_i] = \textstyle\sum_{j=1}^{M} v_j \mathbb{E}[Z_j Y_i] = 0 \end{aligned}$$

where we have used the fact that $u_{R,M|_{\partial D}} = g_M$ a.s. and the random modes are mutually orthogonal. Then the fact that $v_1, ..., v_M$ are linearly independent implies that $\{U_1, ..., U_R, V_1, ..., V_M\}$ are linearly independent. ■

Proof (Lemma 3.1). The fact that $\mathcal{M}_{R,M} \subseteq \mathcal{M}_S^{g_M}$ follows directly from Lemma 3.2. Now we need to show that $\mathcal{M}_S^{g_M} \subseteq \mathcal{M}_{R,M}$. Let $u_S \in \mathcal{M}_S^{g_M}$, we have that:

$$\begin{aligned} u_S &= \textstyle\sum_{i=1}^{S} U_i Y_i \\ &= \textstyle\sum_{i=1}^{S} U_i \Pi_{\mathcal{Z}} Y_i + \sum_{i=1}^{S} U_i \Pi_{\mathcal{Z}}^{\perp} Y_i \\ &= \textstyle\sum_{j=1}^{M} \left(\sum_{i=1}^{S} U_i \mathbb{E}[Y_i Z_j] \right) Z_j + \sum_{i=1}^{S} U_i \Pi_{\mathcal{Z}}^{\perp} Y_i \\ &= \textstyle\sum_{j=1}^{M} V_j Z_j + \sum_{i=1}^{S} U_i \Pi_{\mathcal{Z}}^{\perp} Y_i \end{aligned}$$

Since $u_{S|_{\partial D}} = g_M$ and Z_i are orthogonal, we necessary have that $V_{j|_{\partial D}} = v_j$. Moreover, the fact that v_i are linearly independent implies that $V_1, ..., V_M$ are linearly independent. We can write:

$$\langle v_j, u_{S|_{\partial D}} \rangle_{L^2(\partial D)} = \langle v_j, \sum_{i=1}^{M} v_i \rangle_{L^2(\partial D)} Z_i, \tag{29}$$

that implies

$$\sum_{l=1}^{S} \langle v_j, U_{l|_{\partial D}} \rangle_{L^2(\partial D)} Y_l = \langle v_j, \sum_{i=1}^{M} v_i \rangle_{L^2(\partial D)} Z_i. \tag{30}$$

Let $\mathbf{B} \in \mathbb{R}^{M \times M}$, $\mathbf{C} \in \mathbb{R}^{M \times S}$ denote respectively:

$$\mathbf{B}_{ij} = \langle v_j, v_i \rangle_{L^2(\partial D)} \text{ and } \mathbf{C}_{ij} = \langle v_i, U_{j|_{\partial D}} \rangle_{L^2(\partial D)}.$$

Then, equation (30) can be rewritten as:

$$\mathbf{C}\mathbf{Y}^T = \mathbf{M}\mathbf{Z}^T \quad \Rightarrow \mathbf{Z}^T = \mathbf{M}^{-1}\mathbf{C}\mathbf{Y}^T \tag{31}$$

where we use the fact that $v_1, ..., v_M$ are linearly independent. This shows that:

$$\text{span}(Z_1, ..., Z_M) \subset \text{ span}(Y_1, ..., Y_S).$$

In particular there exist $(\tilde{Y}_1, ..., \tilde{Y}_R)$ orthonormal random variables, orthogonal to the subspace spanned by $(Z_1, ..., Z_M)$ such that:

$$\text{span}(Y_1, ..., Y_S) = \text{span}(Z_1, ..., Z_M) \oplus \text{span}(\tilde{Y}_1, ..., \tilde{Y}_R).$$

Hence u_S can be written according to (28), as:

$$u_S = \sum_{j=1}^{M} V_j Z_j + \sum_{i=1}^{R} \tilde{U}_i \tilde{Y}_i$$

where the linear independence of $\tilde{U}_1, ..., \tilde{U}_R$ follows form the fact that u_S is a S-rank random field.

■

In view of Lemma 3.1 we can exploit representation (28) that enables us to derive the boundary conditions for each mode in the DO reduced system. In particular any $u_S \in \mathcal{M}_S^{g_M}$ is written as:

$$u_S = \sum_{i=1}^{S} U_i Y_i$$

where

- $\{Y_1, .., Y_S\}$ are $L^2(\Omega)$-orthonormal random variables;
- $\{U_1, ..., U_R\}$ are linearly independent;
- $U_{i|_{\partial D}} = 0$ for all $i = 1, ..., R$ $(R = S - M)$ and $U_{i|_{\partial D}} = v_i$ for all $i = R + 1, ..., S$;
- $Y_i = Z_i$ for all $i = R + 1, ..., S$;

Observe that:

$$\mathcal{M}_S^{g_M} \cong \mathcal{M}_R \oplus \mathcal{M}_M^{g_M} \tag{32}$$

where we recall that:

$$\mathcal{M}_M^{g_M} = \left\{ u = \sum_{i=1}^{M} U_i Z_i \,\middle|\, u_{|_{\partial D}} = g_M,\, U_i \in H^1(D) \text{ linearly independent} \right\} \subset H^1(D) \otimes L^2(\Omega)$$

and $\mathcal{M}_R$ is the manifold embedded in $H_0^1(D) \otimes \mathcal{Z}^{\perp}$ of all the random fields of rank R. Observe that if $M = 0$ we recover the standard formulation without constraints according to which $\mathcal{M}_S$ is the manifold of all the random fields of rank S that vanish on the boundary. On the other hand, if $M = S$, $\mathcal{M}_S^{g_S}$ reduces to the S dimensional affine subspace, spanned by $Z_1, ..., Z_M$ and the Dynamical Low Rank approximation reduces to a standard Galerkin projection.
We are now ready to define the Dynamical Low Rank variational principle in $\mathcal{M}_S^{g_M}$, i.e. the manifold of all the S rank random fields that satisfy the (approximate) boundary conditions (25). Observe that, in light of (32), for any $u_S \in \mathcal{M}_S^{g_M}$, we have that:

$$\mathcal{T}_{u_S} \mathcal{M}_S^{g_M} \cong \mathcal{T}_{u_R} \mathcal{M}_R \oplus \left(\mathcal{Z} \otimes H_0^1(D) \right) \tag{33}$$

where $u_R = \Pi^{\perp}_{\mathcal{Z}}[u_S]$. Assuming that we adopt a parametrization of the manifold such that $u_S \in \mathcal{M}_S^{g_M}$ is represented as $\sum_{i=1}^{S} U_i Y_i$ where the last M random variables coincide with $Z_1, .., Z_M$ in (25), then the tangent space can be parametrized as:

$$\mathcal{T}_{u_S}\mathcal{M}_S^{g_M} \cong \Big\{ \dot{u} = \textstyle\sum_{i=1}^{S} \left(\delta U_i Y_i + U_i \delta Y_i\right) \in H_0^1(D) \otimes L^2(\Omega) \text{ s.t.} \quad \mathbb{E}[\delta Y_i Y_j] = 0 \quad \forall i,j = 1,...,S \\ \delta Y_i = 0 \text{ a.s.} \quad \forall i = R+1,...,S \Big\} \tag{34}$$

This construction of constrained approximation manifolds can be generalized to Dirichlet boundary conditions which depend on time. In this case the decomposition (25) is time dependent and the approximation manifold changes in time: $\mathcal{M}_S^{g_M(t)} \cong \mathcal{M}_R \oplus \mathcal{M}_M^{g_M(t)}$. The tangent space is defined at each fixed time, according to (34). Formally the LR variational principle reads the same as in (12). What changes is the definition of the manifold. We project the governing equation into the tangent space to $\mathcal{M}_S^{g_M(t)}$ at $u_S(t)$ at each time where now $\mathcal{M}_S^{g_M(t)}$ is the manifold constrained to $g_M(t)$ which may change in time, hence the approximate solution $u_S(t)$ automatically satisfies the Dirichlet boundary conditions of the original problem.
According to the parametrization of the tangent space in (34) the reduced order system for the Dual DO formulation under random boundary constraints becomes:

$$\dot{U}_i(x,t) = \mathbb{E}\left[\mathcal{L}(u_S(x,t,\cdot))Y_i(t,\cdot)\right] \qquad x \in D,\, t \in (0,T],\, i = 1,\cdots,S \tag{35}$$

$$U_i(x,t) = 0 \qquad (x,t) \in \partial D \times (0,T],\, i = 1,\cdots,R \tag{36}$$

$$U_i(x,t) = v_i(x,t) \qquad (x,t) \in \partial D \times (0,T],\, i = R+1,\cdots,S \tag{37}$$

$$\sum_{j=1}^{R} \mathbf{M}_{ji}(t)\dot{Y}_j(t,\omega) = \Pi^{\perp}_{\mathcal{Y}} \left\langle \mathcal{L}(u_S(\cdot,t,\omega),\omega), U_i(\cdot,t)\right\rangle \qquad (t,\omega) \in (0,T] \times \Omega,\, i = 1,\cdots,R \tag{38}$$

$$\dot{Y}_i(t,\omega) = 0 \qquad (t,\omega) \in (0,T] \times \Omega,\, i = R+1,\cdots,S \tag{39}$$

where $\mathcal{Y}$ =span$(Y_1,...,Y_S)$ and $\mathbf{M} \in \mathbb{R}^{R\times R}$ is the correlation matrix of the first R deterministic modes $\mathbf{M}_{i,j} =< U_i, U_j >$ for $i,j = 1,...,R$. Observe that the system (38) consists of only $R = S - M$ equations since the last M random variables remain constant.

Remark 2. *Again, since in our context of partial differential equations with random parameters we are usually interested in computing the statistics of the solution it may be worth approximating separately the mean of the solution as in (18). Observe that we can distinguish two cases:*

- *(non homogeneous) deterministic boundary conditions. In this case isolating the mean only reduces to a special case of the Dual DO formulation under boundary constraints with $S+1$ modes and $M = 1$ constraint: $\bar{u}_{S+1}$ satisfies the constraints and all other deterministic modes are homogeneous on the boundary. The approximation manifold can be defined including the mean, by taking $U_{S+1} = \bar{u}_{S+1}$ and $Y_{S+1} = 1$. Observe that the non homogeneous boundary conditions guarantee that U_{S+1} and U_i are linearly independent for any $i = 1,...,S$. In practice we work in a manifold of rank $S+1$ under one constraint given by $Y_{S+1} = 1$ at each time.*
- *random boundary conditions. Consider a boundary datum $g = \bar{g} + \sum_{i=1}^{M} v_i Z_i$, with $\mathbb{E}[Z_i] = 0$ and $\bar{g} = \mathbb{E}[g]$, if $\bar{g}$ is linearly independent from $\{v_1,...,v_M\}$ we fall back to the first case, namely isolating the mean coincides with defining the constrained approximation manifold by including the mean: we have $S+1$ linearly independent modes and $M+1$ constraints. On the other hand in the general case, isolating the mean does not guarantee any kind of orthogonality for $\bar{u}_S$ with respect to the other deterministic modes, thus the constrained set which includes the mean is not necessarily a manifold. If*

$\bar{g}$ is not linearly independent from $v_1, ..., v_M$, we can either isolate the mean and work in a manifold of dimension S embedded in $H^1(D) \otimes L^2_0(\Omega)$, either not and write g_M as in 25. Observe that in the first case the approximate solution is in $H^1(D) \oplus \mathcal{M}_S^{g_M}$ and has rank at least equal to S.

An alternative strategy for dealing with random boundary conditions was proposed in [38], [39] and consists in projecting the boundary conditions $g(x,t,\omega)$ onto $\mathcal{Y}(t) = \text{span} < Y_1, ..., Y_S >$ at each t. Combining this approach to the Dual DO framework would imply enforcing:

$$U_i(x,t)_{|_{\partial D}} = \mathbb{E}[g(x,t,\cdot)Y_i(t,\cdot)] \quad \forall x \in \partial D, \forall t \in (0,T], \forall i = 1, ..., S$$

which further implies:

$$u_S(x,t,\cdot)_{|_{\partial D}} = \sum_{i=1}^{S} \mathbb{E}[g(x,t,\cdot)Y_i(t,\cdot)]Y_i(t,\omega) \quad \forall x \in \partial D, \forall t \in (0,T], \forall i = 1, ..., S.$$

However, note that the subspace spanned by $Y_1, ..., Y_S$ evolves in time and it is implicitly determined by the approximate solution itself. It is not clear then at time $t \gg 0$ which boundary conditions are actually satisfied by u_S and how the randomness arising from the boundary data is taken into consideration. The two different strategies are numerically compared in Section 5. The results for the problems under analysis show that strong imposition of boundary constrains leads to better performances in terms of accuracy versus number of modes, especially for long time intervals.

3.3 Best S rank approximation

We now look at the problem of finding the best S rank approximation in $\mathcal{M}_S^{g_M(t)}$ at any fixed time $t \in [0,T]$.This can be seen as an optimization problem under constraints.

Definition 3.3. *Fix $t \in [0,T]$ and let $u(t) \in H^1(D) \otimes L^2(\Omega)$ be a square integrable random field with rank greater or equal to S and such that $u(x,t,\omega) = g_M(x,t,\omega)$ for all $x \in \partial D$ a.s.. We define best rank S approximation a solution of the following problem: find $u_S^{KL}(t) \in \mathcal{M}_S^{g_M(t)}$ such that*

$$u_S^{KL}(t) = \underset{v_S \in \mathcal{M}_S^{g_M(t)}}{\text{argmin}} \|u(t) - v_S\|_{L^2(D) \otimes L^2(\Omega)} \tag{40}$$

Lemma 3.3. *The solution to problem (40) is given by:*

$$\begin{aligned} u_S^{KL}(x,t,\omega) &= \textstyle\sum_{i=1}^{R} \sqrt{\lambda_i(t)} V_i^{KL}(x,t) Z_i^{KL}(t,\omega) + \sum_{i=1}^{M} V_i(x,t) Z_i(\omega,t) \\ &= u_R^{KL}(t) + \underbrace{\sum_{i=1}^{M} V_i(x,t) Z_i(t,\omega)}_{u_M^*(t)} \end{aligned} \tag{41}$$

where

- *$u_M^*(t) \in \mathcal{M}_M^{g_M(t)}$ is the Galerkin projection of $u(t)$ in $H^1(D) \otimes \mathcal{Z}(t)$. Specifically $V_i(x,t) = \mathbb{E}[u(x,t,\cdot)Z_i(t,\cdot)]$;*
- *$u_R^{KL}(t)$ is the best approximation with R terms of $\Pi^{\perp}_{\mathcal{Z}(t)}[u(t)] = u(t) - u_M^*(t)$: $(\lambda_i(t), V_i^{KL}(t), Z_i^{KL}(t))_{i=1}^{R}$ are the first R terms of the Karhunen-Loève expansion of $\Pi^{\perp}_{\mathcal{Z}(t)}[u(t)]$.*

Proof. Observe that $\mathcal{M}_S^{g_M(t)} \subset H^1(D) \otimes L^2(\Omega)$ while the minimization in (40) is defined in $L^2(D) \otimes L^2(\Omega)$. In order to formally recover the constraint (26), i.e. $u_S^{KL}(x,t,\omega) = g_M(x,t,\omega)$, $\forall x \in \partial D$ a.s., we set problem (40) in the larger space $\mathcal{V} \subset L^2(D) \otimes L^2(\Omega)$ defined as:

$$\mathcal{V} = L^2(D) \otimes \mathcal{Z}(t) \oplus \mathcal{M}_R(L^2(D) \otimes \mathcal{Z}^{\perp}(t))$$

where $\mathcal{M}_R(L^2(D) \otimes \mathcal{Z}^{\perp}(t))$ is the manifold of R rank random fields embedded in $L^2(D) \otimes \mathcal{Z}^{\perp}(t)$. Now let us define the following problem: *F*ind $\tilde{u}_S^{KL}(t) \in \mathcal{V}$ such that

$$\tilde{u}_S^{KL}(t) = \underset{v_S \in \mathcal{V}}{\operatorname{argmin}} \|u(t) - v_S\|_{L^2(D) \otimes L^2(\Omega)} \tag{42}$$

The problem (42) reduces to two well known problems: a Galerkin projection in $\mathcal{Z}(t)$ plus an optimization problem without constraints in $\mathcal{M}_R(L^2(D) \otimes \mathcal{Z}^{\perp}(t))$. This implies that problem (42) is well posed and admits a solution $\tilde{u}_S^{KL}(t)$ that can be written as in (41). Moreover observe that $\tilde{u}_S^{KL}(t) \in \mathcal{M}_S^{g_M(t)} \subset \mathcal{V}$, which implies that $\tilde{u}_S^{KL}(t) = u_S^{KL}(t)$ is a solution of problem (42). ■

In the following we call best S rank approximation $u_S^{KL}(t)$ the solution to problem (40).

Remark 3. *The error analysis derived in [32] for linear parabolic equations with random parameters applies as well to the Dual DO approximation under constraints. In this case the DLR approximation error is bounded in term of the best approximation (41), i.e. the solution of the optimization problem under constraints (40). The proof follows very closely the one derived in [32].*

4 Application to Navier Stokes equations

In this Section we focus on fluid flow dynamics governed by the non-stationary Navier Stokes equations for incompressible, constant-density fluids. In this setting the uncertainty may arise from the parameters of the equations such as the fluid viscosity, or from the forcing term or initial or boundary conditions. The general problem, in a open, bounded Lipschitz domain $D \subset \mathbb{R}^d$, with $d = 2, 3$, reads a.s. in Ω as:

$$\begin{cases} \dot{\mathbf{u}}(\mathbf{x},t,\omega) - \nu(\mathbf{x},t,\omega)\Delta\mathbf{u}(\mathbf{x},t,\omega) + \mathbf{u}(\mathbf{x},t,\omega)\cdot\nabla\mathbf{u}(\mathbf{x},t,\omega) + \nabla p(\mathbf{x},t,\omega) = \mathbf{f}(\mathbf{x},t,\omega) & (\mathbf{x},t) \in D \times (0,T] \\ \nabla \cdot \mathbf{u}(\mathbf{x},t,\omega) = 0 & \\ \mathbf{u}(\mathbf{x},0,\omega) = \mathbf{u}_0(\mathbf{x},\omega) & \mathbf{x} \in D \\ \mathbf{u}(\mathbf{x},t,\omega) = \mathbf{g}(\mathbf{x},t,\omega) & \mathbf{x} \in \Gamma_D,\ t \in (0,T] \\ \nu\partial_{\mathbf{n}}\mathbf{u}(\mathbf{x},t,\omega) - p(\mathbf{x},t,\omega)\cdot\mathbf{n} = \mathbf{h}(\mathbf{x},t,\omega) & \mathbf{x} \in \Gamma_N,\ t \in (0,T] \end{cases} \tag{43}$$

where $\mathbf{u}$ is the velocity (column) vector field, p is the scalar pressure and ν is the kinematic viscosity that may eventually be modeled as a random variable or random field. Γ_D and Γ_N are disjointed parts of the boundary ∂D, such that $\overline{\Gamma}_D \cup \overline{\Gamma}_N = \partial D$, on which we impose Dirichlet and Neumann boundary conditions respectively. Our goal is to find a low rank approximation of the velocity field. We apply the Dual DO method described in Section 3 and we derive evolution equations for all the factors $(\mathbf{U}, \mathbf{Y})$ of the approximate velocity vector field. We start by recalling the definition of Karhunen-Loève expansion for a square integrable random *vector* field.

Definition 4.1. *Let* $\mathbf{u} \in L^2\big(\Omega, [L^2(D)]^d\big)$ *be a square integrable random field with covariance function* $\mathrm{Cov}_{\mathbf{u}} : D \times D \to \mathbb{R}^{d\times d}$*, defined as:*

$$\mathbf{Cov}_{\mathbf{u}}(\mathbf{x},\mathbf{y}) = \mathbb{E}[\mathbf{u}^*(\mathbf{x},\cdot)\mathbf{u}^{*\mathrm{T}}(\mathbf{y},\cdot)]$$

with $\mathbf{u}^* = \mathbf{u} - \mathbb{E}[\mathbf{u}]$.
Then $\mathbf{u}$ *can be written as:*

$$\mathbf{u}(\mathbf{x},\omega) = \bar{\mathbf{u}}(\mathbf{x},\omega) + \underbrace{\sum_{i=1}^{\infty} \sqrt{\lambda_i}\mathbf{V}_i^{KL}(\mathbf{x})Z_i^{KL}(\omega)}_{\mathbf{u}^*} \tag{44}$$

where:

- $\{\lambda_i, \mathbf{V}_i^{KL}\}$ *are respectively the (non-zero) eigenvalues and eigenfunctions (column vectors of scalar functions) of the covariance operator* $T_{\mathbf{u}} : [L^2(D)]^d \to [L^2(D)]^d$ *defined as*

$$T_{\mathbf{u}}\mathbf{V}(\mathbf{x}) = \int_D \mathbf{Cov}_{\mathbf{u}}(\mathbf{y},\mathbf{x})\mathbf{V}(\mathbf{y})\mathrm{d}\mathbf{y}, \quad \mathbf{V} \in [L^2(D)]^d \tag{45}$$

$$T_{\mathbf{u}}\mathbf{V}_i^{KL} = \lambda_i \mathbf{V}_i^{KL} \tag{46}$$

- Z_i^{KL} *are mutually uncorrelated scalar random variables given by:*

$$Z_i^{KL}(\omega) := \frac{1}{\sqrt{\lambda_i}} \int_D (\mathbf{u}^*(x,\omega))^T \mathbf{V}_i^{KL}(x)dx \qquad \forall i \in \mathbb{N}^+, \tag{47}$$

  with zero mean and unit variance.

Observe that the deterministic modes are vector valued functions while the stochastic modes are scalar functions. We denote by $H^1_{div}(D)$ and $H^1_{\Gamma_D}(D)$ the following spaces:

$$H^1_{div}(D) := \big\{\mathbf{v} \in [H^1(D)]^d \,:\, \nabla\cdot\mathbf{v} = 0\big\},$$

$$H^1_{\mathbf{g}}(D) := \big\{\mathbf{v} \in [H^1(D)]^d \,:\, \mathbf{v}_{|\Gamma_D} = \mathbf{g}\big\}, \quad H^1_{\Gamma_D}(D) := \big\{\mathbf{v} \in [H^1(D)]^d \,:\, \mathbf{v}_{|\Gamma_D} = \mathbf{0}\big\}.$$

Remark 4. *Let* $\mathbf{u}$ *be in* $H^1_{div}(D) \otimes L^2(\Omega)$*, then the mean and all the deterministic eigen-modes in (44) are divergence free. Indeed*

$$\nabla\cdot\bar{\mathbf{u}} = \nabla\cdot\mathbb{E}[\mathbf{u}] = \mathbb{E}[\nabla\cdot\mathbf{u}] = 0, \qquad \lambda_i\nabla\cdot\mathbf{V}_i^{KL} = \nabla\cdot\mathbb{E}[\mathbf{u}Z_i^{KL}] = \mathbb{E}[\big(\nabla\cdot\mathbf{u}\big)Z_i^{KL}] = 0$$

In light of Remark 4, we look for a Dynamical Low Rank approximation written as a linear combination of divergence free modes. We consider the general case of problem (43) with random Dirichlet boundary conditions, and detail the Dual DO formulation introduced in Section 3.1 in which we also isolate the mean. Following the discussion in Section 3.2, we assume that the datum on the Dirichlet boundary can be properly approximated by a M rank random field, with $M \leq S$. In particular, for consistency with the approximate solution, the boundary constraint is decomposed according to Definition (18), by isolating the mean:

$$\mathbf{u}(\mathbf{x},t,\omega) = \mathbf{g}(\mathbf{x},t,\omega) \approx \mathbf{g}_M(\mathbf{x},t,\omega) = \bar{\mathbf{g}}(\mathbf{x},t) + \mathbf{g}^*_M(\mathbf{x},t,\omega), \quad \mathbf{x} \in \Gamma_D,\, t \in [0,T],\ \text{a.s.} \tag{48}$$

Hence $\bar{\mathbf{g}}(\mathbf{x},t)$ is the deterministic Dirichlet boundary condition for the mean, while $\mathbf{g}^*_M(\mathbf{x},t,\omega)$, written as a linear combination of $M \leq S$ zero mean random variables, is the constraint of the approximation manifold. To be precise:

$$\mathbf{g}_M(\mathbf{x},t,\omega) = \bar{\mathbf{g}}(\mathbf{x},t) + \sum_{i=1}^{M} \boldsymbol{v}_i(\mathbf{x},t)Z_i(t,\omega), \quad \forall \mathbf{x} \in \Gamma_D,\, t \in [0,T],\ \text{a.s.} \tag{49}$$

with:

- $Z_1, ..., Z_M$ zero mean $L^2(\Omega)$-orthonormal random variables: $\mathbb{E}[Z_i(\cdot,t)] = 0$, $\mathbb{E}[Z_i(\cdot,t)Z_j(\cdot,t)] = \delta_{ij}$ for all $i, j = 1, ..., M$
- $\boldsymbol{v}_1, ..., \boldsymbol{v}_M$ linearly independent vector valued deterministic functions.

and the approximation manifold of *zero mean* S rank random fields constrained to $\mathbf{g}_M^*(t)$ is parametrized as follows:

$$\boldsymbol{\mathcal{M}}_{S,div}^{\mathbf{g}_M^*(t)} = \Big\{ \mathbf{u}_S^* = \textstyle\sum_{i=1}^S \mathbf{U}_i Y_i \text{ s.t.} \quad \mathbf{u}_{S|_{\Gamma_D}} = \mathbf{g}_M^*(t), \text{ and } \mathbf{U}_i \in H_{div}^1(D), \\ \mathbb{E}[Y_i] = 0,\, \mathbb{E}[Y_i Y_j] = \delta_{ij}, \text{ rank}(\mathbf{M}) = R \Big\} \tag{50}$$

where $R = S - M$ and $\mathbf{M} =\ll \mathbf{U}, \mathbf{U} \gg \in \mathbb{R}^{R\times R}$ is again the full rank correlation matrix of the first R deterministic modes: $\mathbf{M}_{ij} =< \mathbf{U}_i, \mathbf{U}_j >= \sum_{k=1}^d < U_{i,k}, U_{j,k} >$. Thus, the DLR approximate solution is written at each time as:

$$\mathbf{u}_S(t) = \bar{\mathbf{u}}_S(t) + \mathbf{u}_S^*(t)$$

with:

- $\bar{\mathbf{u}}_S(t) \in H_{div}^1(D) \cap H_{\bar{\mathbf{g}}(t)}^1(D)$,
- $\mathbf{u}_S^*(t) \in \boldsymbol{\mathcal{M}}_{S,div}^{\mathbf{g}_M^*(t)}$.

Finally, the DLR variational principle (12) applied to the Navier Stokes problem in (43) becomes:

Proposition 4.1. *At each time t, find* $(\bar{\mathbf{u}}_S(t), \mathbf{u}_S^*(t)) \in (H_{div}^1(D) \cap H_{\bar{\mathbf{g}}(t)}^1(D)) \times \boldsymbol{\mathcal{M}}_{S,div}^{\mathbf{g}_M^*(t)}$ *such that* $\mathbf{u}_S(t) = \bar{\mathbf{u}}_S(t) + \mathbf{u}_S^*(t) = \bar{\mathbf{u}}_S(t) + \sum_{i=1}^S \mathbf{U}_i(t) Y_i(t)$ *satisfies:*

$$\mathbb{E}\big[< \dot{\mathbf{u}}_S + \mathbf{u}_S \cdot \nabla \mathbf{u}_S - \mathbf{f},\, \mathbf{v} > + < \nu \nabla \mathbf{u}_S, \nabla \mathbf{v} > - < \mathbf{h}, \mathbf{v} >_{\Gamma_N} \big] = 0 \\ \forall \mathbf{v} \in (H_{div}^1(D) \cap H_{\Gamma_D}^1(D)) \times \mathcal{T}_{\mathbf{u}_S(t)} \boldsymbol{\mathcal{M}}_{S,div}^{\mathbf{g}_M^*(t)}. \tag{51}$$

with initial condition given by $\bar{\mathbf{u}}(0) + \mathbf{u}_S^*(0)$, *where* $\bar{\mathbf{u}}(0) = \mathbb{E}[\mathbf{u}_0]$ *and* $\mathbf{u}_S^*(0)$ *is the best* S *rank approximation of* $\mathbf{u}_0 - \bar{\mathbf{u}}(0)$ *in* $\boldsymbol{\mathcal{M}}_{S,div}^{\mathbf{g}_M^*(0)}$, *provided* $\mathbf{u}_0 \in H_{div}^1 \otimes L^2(\Omega)$.

Observe that the term $< \mathbf{h}, \mathbf{v} >_{\Gamma_N}$ derives from the integration by part of $-\nu < \Delta \mathbf{u}_S, \mathbf{v} > + < \nabla p, \mathbf{v} >$ combined with the Neumann boundary conditions in Γ_N. Again, by imposing condition (14), we can equip $\boldsymbol{\mathcal{M}}_{S,div}^{\mathbf{g}_M^*(t)}$ with a differential manifold structure and derive the Dual DO reduced order system for Navier Stokes equations with random parameters (including boundary conditions).

Proposition 4.2. *Let* $(\bar{\mathbf{u}}_S, \mathbf{U}, \mathbf{Y})$ *be a smooth solution of*

$$\begin{cases} < \dot{\bar{\mathbf{u}}}_S + \mathbb{E}\big[\mathbf{u}_S \cdot \nabla \mathbf{u}_S - \mathbf{f}\big],\, \delta\mathbf{U} > + < \mathbb{E}\big[\nu \nabla \mathbf{u}_S\big],\, \nabla \delta \mathbf{U} > - < \mathbb{E}\big[\mathbf{h}\big], \delta \mathbf{U} >_{\Gamma_N} = 0 \\ \bar{\mathbf{u}}_{S_{|\Gamma_D}} = \bar{\mathbf{g}} \\ < \dot{\mathbf{U}}_i + \mathbb{E}\big[\big(\mathbf{u}_S \cdot \nabla \mathbf{u}_S - \mathbf{f}\big) Y_i\big],\, \delta\mathbf{U} > + < \mathbb{E}\big[\nu \nabla \mathbf{u}_S Y_i\big],\, \nabla \delta \mathbf{U} > - < \mathbb{E}\big[\mathbf{h} Y_i\big], \delta \mathbf{U} >_{\Gamma_N} = 0 \\ \mathbf{U}_{i|\Gamma_D} = 0 \qquad \forall i = 1, ..., R \\ \mathbf{U}_{i|\Gamma_D} = \boldsymbol{v}_i \qquad \forall i = R+1, ..., S \\ \\ \sum_{k=1}^R \mathbf{M}_{jk} \mathbb{E}[\dot{Y}_k \delta Y] =< \mathbf{U}_j, \mathbb{E}\big[\big(\mathbf{f} - \mathbf{u}_S \cdot \nabla \mathbf{u}_S\big)\delta Y\big] > - < \nabla \mathbf{U}_j, \mathbb{E}\big[\nu \nabla \mathbf{u}_S \delta Y\big] > + < \mathbf{U}_j, \mathbb{E}\big[\mathbf{h} \delta Y\big] >_{\Gamma_N} \\ \qquad \forall j = 1, ..., R \end{cases} \tag{52}$$

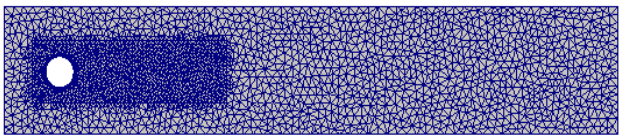

Figure 1: Left: mesh used for the simulation, 2592 number of vertices, h_{max}= 0.055, h_{min}=0.006.

$\forall \delta \mathbf{U} \in H^1_{div}(D) \cap H^1_{\Gamma_D}(D)$ and $\forall \delta Y \in \mathcal{Y}_0^{\perp}$ (the orthogonal complement of $\mathcal{Y}$ in $L^2_0(\Omega)$), with initial conditions given by $\bar{\mathbf{u}}(0)$ and the best S rank approximation of $\mathbf{u}_0 - \bar{\mathbf{u}}(0)$ in $\boldsymbol{\mathcal{M}}^{\mathbf{g}^*_M(0)}_{S,div}$. Then $\mathbf{u}_S = \bar{\mathbf{u}}_S + \sum_{i=1}^S \mathbf{U}_i Y_i$ is solution of (51), at each time.

We treat the divergence free constraint, that is imposed on each deterministic mode, by introducing $S+1$ Lagrange multipliers $\bar{p}$, $p_1, ..., p_S$. Then, by reintegrating by part, we finally get:

Proposition 4.3. *Let $(\bar{\mathbf{u}}_S, \mathbf{U}, \mathbf{Y})$ be a smooth solution of*

$$
\begin{array}{ll}
\dot{\bar{\mathbf{u}}}_S + \nabla \bar{p} = \mathbb{E}\big[\nu \Delta \mathbf{u}_S - \mathbf{u}_S \cdot \nabla \mathbf{u}_S + \mathbf{f}\big] & \\
\nabla \cdot \bar{\mathbf{u}}_S = 0 & \\
\dot{\mathbf{U}}_i + \nabla p_i = \mathbb{E}\big[\big(\nu \Delta \mathbf{u}_S - \mathbf{u}_S \cdot \nabla \mathbf{u}_S + \mathbf{f}\big) Y_i\big] & \\
\nabla \cdot \mathbf{U}_i = 0 & \forall i = 1, ..., S \\
\sum_{k=1}^R \mathbf{M}_{ik} \dot{Y}_k = < \mathbf{U}_i, \Pi^{\perp}_{1 \cup \mathcal{Y}} \big[\nu \Delta \mathbf{u}_S - \mathbf{u}_S \cdot \nabla \mathbf{u}_S + \mathbf{f}\big] > & \forall i = 1, ..., R
\end{array}
\tag{53}
$$

then $\mathbf{u}_S = \bar{\mathbf{u}}_S + \mathbf{U}\mathbf{Y}$ is solution of (51), at each time.
The initial conditions are given by $\bar{\mathbf{u}}(0)$ and the best S rank approximation of $\mathbf{u}_0 - \bar{\mathbf{u}}(0)$ in $\boldsymbol{\mathcal{M}}^{\mathbf{g}^*_M(0)}_{S,div}$, while the boundary conditions are the following:

$$
\begin{array}{ll}
\bar{\mathbf{u}}_S(x,t) = \bar{\mathbf{g}}(x,t) & (\mathbf{x},t) \in \Gamma_D \times [0,T], \\
\mathbf{U}_i(x,t) = \boldsymbol{v}_i(x,t) & (\mathbf{x},t) \in \Gamma_D \times [0,T],\ \forall i = 1, ..., R \\
\mathbf{U}_i(x,t) = \mathbf{0} & (\mathbf{x},t) \in \Gamma_D \times [0,T],\ \forall i = R+1, ..., S \\
\nu \partial_{\mathbf{n}} \mathbf{U}_i(\mathbf{x},t) - p_i(\mathbf{x},t) \cdot \mathbf{n} = \mathbb{E}[\mathbf{h}(\mathbf{x},t,\cdot) Y_i] & (\mathbf{x},t) \in \Gamma_N \times [0,T],\ \forall i = 1, ..., S.
\end{array}
$$

In conclusion, the Navier Stokes equations with random parameters in (43) is reduced to S deterministic problems of Navier Stokes type, coupled to a system of R stochastic ODEs.

5 Numerical Test

5.1 Flow around a cylinder: stochastic boundary condition

In this section we consider a two-dimensional incompressible flow over a circular cylinder at moderate Reynold's Numbers for which a periodic vortex shedding phenomenon is observed around the obstacle. The geometry and the mesh used for the simulations are shown in Figure 1. The height and length of the channel are respectively $H = 0.41$ and $l = 2.2$. The cylinder hole has radius $r = 0.05$ and is slightly uncentered, the coordinate of the center being $(0.2,\ 0.2)$ with respect to the origin located on the lower-left corner of the channel. We consider homogeneous initial conditions and we assume a parabolic inflow profile with random

peak velocity U_{max} that varies in the range $[1.2, 1.8]$. More precisely we have:

$$\begin{aligned}\mathbf{u}(\mathbf{x},\omega,t) &= (4\underbrace{(\bar{U}+\sigma Z(\omega))}_{U_{max}}x_2(H-x_2)/H^2,\,0) \qquad\qquad \mathbf{x}=(x_1,x_2)\in\Gamma_{in}\\ &= (4\bar{U}x_2(H-x_2)/H^2,\,0)+(4\sigma Z(\omega)x_2(H-x_2)/H^2,\,0)\\ &= \bar{\mathbf{g}}(\mathbf{x})+\underbrace{Z(\omega)\boldsymbol{v}_1(\mathbf{x})}_{\mathbf{g_1}}\end{aligned} \tag{54}$$

where $\bar{U}=1.5$, $\sigma=0.1$ and Z is a uniform random variable with zero mean and unit variance. An initial ramp is applied on the boundary data to guarantee consistency with the homogeneous initial conditions. We use a cubic polynomial smoothing function that reaches 1 at time t=1. No slip conditions are applied on the top, bottom and cylinder side-walls, Neumann homogeneous conditions at the outlet. We recall that for this problem the Reynold's number (that can be computed as $Re=\frac{U_m D}{\nu}$ where here $\nu=10^{-3}$ is the kinematic viscosity and $U_m=\frac{2}{3}U_{max}$ is the mean inflow velocity) determines the frequency of the vortex shedding and the length of the recirculation region. Observe that the random boundary condition at the inflow directly influences the Reynold's Numbers, that here varies in the range $Re\in[80,120]$. It follows that the pattern of the solutions corresponds to flows with random vortex shedding frequency. Before presenting the numerical results we remark that even if we have only one random variable as input, the problem is not straightforward, since the solution depends non-linearly on it. Indeed the test case under consideration is challenging for model order reduction techniques, which are unable to approximate the solution manifold with a relatively small number of modes. This is due to the fact that each value of the input parameter leads to a vortex shedding with different frequency and characteristic length. Somehow we can imagine the manifold of solutions to be constituted of infinitely many flow patterns which become more and more out of phase one with respect to the others as time evolves. Consequently, even if we start with a low rank initial condition (or even deterministic) the rank of the solution will significantly increase in time. This can be verified by looking at the evolution of the eigeinvalues of the covariance operator in Figure 8 (left). Consider for instance the POD method [3] [5], in which the approximate solution is sought as a linear combination of (deterministic and fixed in time) precomputed modes. For a fixed value of Reynold's number the solution is periodic and the vortex shedding can be well reproduced as a linear combination of few pairs of modes with alternating symmetry properties: the dynamics of the solution is approximately low rank (or well approximated in a low dimensional manifold), at least once the vortex shedding is fully developed. On the other hand it has been shown (see for instance [33] [28] for details), that the span of the eigen-modes changes significantly with the Reynold's number, making the POD approach very sensitive to the choice of the parameters used to compute the snapshots. Indeed POD techniques may fail to capture the dynamics for values of the Reynold's number different from those used to pre-compute the modes. We are interested in understanding if the dynamical approach of the DLR method can, at least partially, overcome this problem. In particular we analyze the performance of the Dual DO method in describing both the transient period and the long term periodic dynamics.

5.1.1 Dual DO system and numerical discretization

We apply the Dual DO formulation to the Navier Stokes (NS) equations derived in Section 4. By isolating the mean, the Dual DO approximate solution is written as:

$$\mathbf{u}_S(\mathbf{x},t,\omega)=\bar{\mathbf{u}}_S(\mathbf{x},t)+\sum_{i=1}^{S-1}\mathbf{U}_i(\mathbf{x},t)Y_i(t,\omega)+\mathbf{U}_S(\mathbf{x},t)Z(\omega)$$

where Z is the random variable in (54), and $\mathbf{u}_S^* = \mathbf{u}_S - \bar{\mathbf{u}}_S$ belongs to the low dimensional manifold:

$$\mathcal{M}_{S,div}^{\mathbf{g}_1(t)} = \left\{ \mathbf{u}_S = \sum_{i=1}^{S} \mathbf{U}_i Y_i \text{ s.t. } \mathbf{u}_{S|_{\Gamma_{in}}} = \mathbf{g_1}(t),\, \mathbf{U}_i \in H^1_{div},\, Y_i \in L^2_0(\Omega),\, \mathbb{E}[Y_i Y_j] = \delta_{ij},\ \text{rank}(\mathbf{M}) = S-1 \right\}$$

Let $\mathbb{B}$ denote the third order tensor defined as $\mathbb{B}_{ijk} := \mathbb{E}[Y_i Y_j Y_k]$, the Dual DO system for this problem reads:

$$\begin{cases} \dot{\bar{\mathbf{u}}}_S - \nu \Delta \bar{\mathbf{u}}_S + \bar{\mathbf{u}}_S \cdot \nabla \bar{\mathbf{u}}_S + \sum_{i=1}^{S} \mathbf{U}_i \cdot \nabla \mathbf{U}_i + \nabla \bar{p}_S = 0 \\ \nabla \cdot \bar{\mathbf{u}}_S = 0 \\ \bar{\mathbf{u}}_{S|_{\Gamma_{in}}} = \bar{\mathbf{g}} \end{cases} \tag{55}$$

$$\begin{cases} \dot{\mathbf{U}}_k - \nu \Delta \mathbf{U}_k + \sum_{i=1}^{S}\sum_{j=1}^{S} \mathbb{B}_{ijk} \mathbf{U}_i \cdot \nabla \mathbf{U}_j + \mathbf{U}_k \cdot \nabla \bar{\mathbf{u}}_S + \bar{\mathbf{u}}_S \cdot \nabla \mathbf{U}_k + \nabla p_k = 0 \qquad k = 1, ..., S \\ \nabla \cdot \mathbf{U}_k = 0 \\ \mathbf{U}_{1|_{\Gamma_{in}}} = \boldsymbol{v}_1 \qquad \mathbf{U}_{k|_{\Gamma_{in}}} = \mathbf{0} \qquad \text{for } k \neq 1 \end{cases} \tag{56}$$

$$\sum_{i=1}^{S-1} \mathbf{M}_{ki} \dot{Y}_i + \Pi^{\perp}_{1 \cup \mathcal{Y}} < \mathbf{U}_k, \sum_{i=1}^{S}\sum_{j=1}^{S} \mathbf{U}_i \cdot \nabla \mathbf{U}_j > Y_i Y_j = 0 \qquad k = 1, ..., S-1 \tag{57}$$

$$Y_S = Z \tag{58}$$

No slip conditions on the top, bottom and cylinder side-walls and homogeneous Neumann boundary conditions on the outflow are applied for $\bar{\mathbf{u}}_S, \mathbf{U}_1, ..., \mathbf{U}_S$. Observe that the Dual DO system (55)-(58) reduces to $S+1$ (coupled) Navier Stokes equations, plus a system of $S-1$ ODEs. However playing with the time discretization it is possible to decouple the system to save computational time and effectively compute the approximate solution without losing the stability. In particular we used a splitting scheme of "Gauss-Seidel" type to linearize and completely decouple the system of ODEs from the system of PDEs. Specifically both the third order tensor $\mathbb{B}$ and the projection operator $\Pi^{\perp}_{1 \cup \mathcal{Y}}(\cdot)$ are treated explicitly whereas the update of the random variables $\{Y_i\}$ is done on the newly computed basis $\{U_i\}$. In particular, denoting by $\mathbf{u}_S^n = \bar{\mathbf{u}}_S^n + \mathbf{U}^n (\mathbf{Y}^n)^T$ the approximate solution at time $t^n = n\Delta t$, equations (55) and (56) are discretized in time as follows:

$$\begin{aligned} &\tfrac{1}{\Delta t} \bar{\mathbf{u}}_S^{n+1} - \nu \Delta \bar{\mathbf{u}}_S^{n+1} + \bar{\mathbf{u}}_S^n \cdot \nabla \bar{\mathbf{u}}_S^{n+1} + \nabla \bar{p}_S^{n+1} = \tfrac{1}{\Delta t} \bar{\mathbf{u}}_S^n - \sum_{i=1}^{S} \mathbf{U}_i^n \cdot \nabla \mathbf{U}_i^n \\ &\tfrac{1}{\Delta t} \mathbf{U}_k^{n+1} - \nu \Delta \mathbf{U}_k^{n+1} + (\bar{\mathbf{u}}_S^n + \sum_{i=1}^{S} \mathbb{B}_{ikk}^n \mathbf{U}_i^n) \cdot \nabla \mathbf{U}_k^{n+1} + \nabla p_k^{n+1} = \tfrac{1}{\Delta t} \mathbf{U}_k^n - \sum_{\substack{j=1 \\ j \neq k}}^{S}\sum_{i=1}^{S} \mathbb{B}_{ijk}^n \mathbf{U}_i^n \cdot \nabla \mathbf{U}_j^n - \mathbf{U}_k^n \cdot \nabla \bar{\mathbf{u}}_S^n \end{aligned}$$

In conclusion at each time step we first solve in parallel $S+1$ decoupled deterministic NS equations and then a system of $S-1$ ODEs. We chose to discretize functions defined in the physical space by a Finite Element method, with P_2 elements for the velocity and P_1 for the pressure, to ensure that the inf-sup condition is satisfied at the discrete level. Then each of the $S+1$ deterministic NS equations system is solved by using the Chorin-Teman projection scheme with rotational incremental pressure correction [42]. The system of ODEs is instead discretized by using the Stochastic Collocation method with Gauss-Legendre points (the stochastic space has been parametrized by a uniform random variable, according with the input data).
The first difficulty in applying the Dual DO method concerns the initialization of the modes. Indeed, the initial condition is deterministic, i.e. a zero rank random field, but the rank is expected to increase in time, due to the randomness in the boundary data and the non linearity of the problem. It follows that we may expect $S > 1$ modes to be needed to effectively describe the dynamics of the solutions. In practice we look

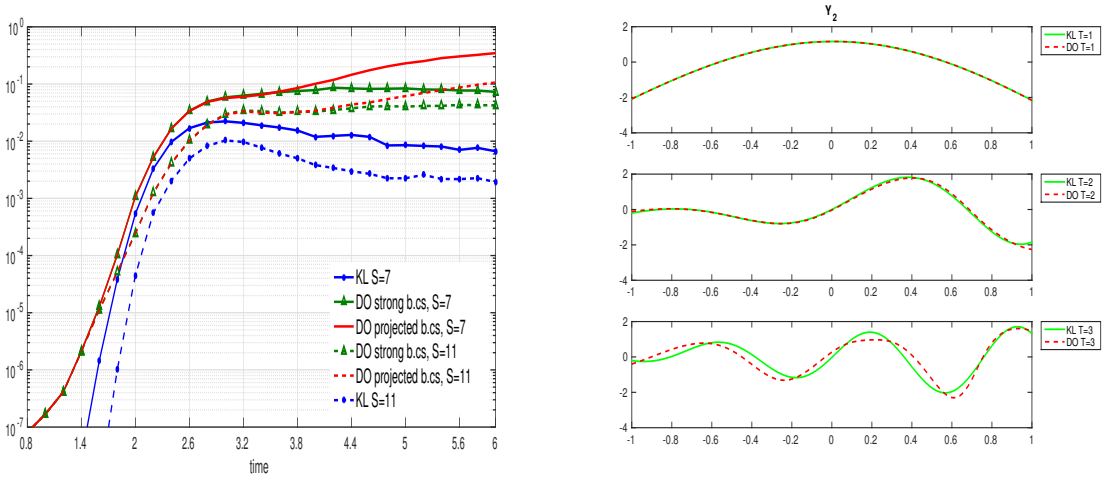

Figure 2: Left: time evolution of the approximation error in norm $H^1(D) \otimes L^2(\Omega)$ with $S = 7$ modes (and $S = 11$, dashed lines). In blue the best approximation error, in red the approximation error of DO method with projected boundary conditions ([38] [39]), in green approximation error of the Dual DO with strong imposition of boundary constraints. Right: The second stochastic mode of the KL decomposition of the reference solution (green) and the DO approximate solution (red dashed line) with $S = 5$ at time $T = 1$, $T = 2$, $T = 3$

for the Dual DO approximate solution $\mathbf{u}_S$ even if the initial condition has clearly defective rank. We initialize the last random mode to Z in (54) and the first $S-1$ to an orthonormal polynomial basis in $Z^{\perp}$, whereas the deterministic modes are set to zero. Observe that $\mathbf{u}_S$ does not belong to the approximation manifold $\mathcal{M}_{S,div}^{\mathbf{g}_1(t)}$ at least at the initial time steps. This is a common problem of DLR methods and may arise even if the initial solution is full rank, because nothing prevent the DLR solution to become rank deficient at some point in time. To treat the case of rank deficiency here we used the same strategy proposed in [32] that consists in diagonalizing the correlation matrix $\mathbf{M}$ at each time step and solving the equations only for the eigen-modes with eigenvalues larger than a prescribed (small) tolerance, whereas the other modes are kept constant in time. By this way, the stochastic coefficients associated to deterministic modes with L^2 norm below the threshold, have a negligible influence on the approximation of the solution. However, they are kept in the approximation and may become active again at a later time when the rank of the solution increases. See [32] for more details. We mention that an alternative strategy to treat rank deficiency is proposed in [26], in the context of time dependent matrices, which makes use of a projector splitting integrator.

Numerical results

First of all we assess the accuracy of the Dual DO formulation with constraints according to which the random boundary conditions are imposed strongly. This technique is compared to the one proposed in [38] that consists in projecting the boundary data in the subspace spanned by the random modes at each time. The approximation error is calculated with respect to the reference solution computed by using the Stochastic Collocation method with Gauss-Legendre points and with the same discretization parameters in time and space. In Figure 2 (left) we compare the approximation error in norm $H^1(D) \otimes L^2(\Omega)$ for the two strategies with S (number of modes) equal to 7 and 11. We observe that for the problem under consideration the strategy proposed here exhibits a smaller error for long time integration. We stress that for this problem the first random mode is fixed and distributed as Z in (54) while the other $S-1$ random modes, initialized to a arbitrary orthonormal basis in the orthogonal complement to Z, "automatically" adapt to the structure of the solution. In Figure 2 (right) and Figure 3 we compare the random modes of the Dual DO approximate solution to the

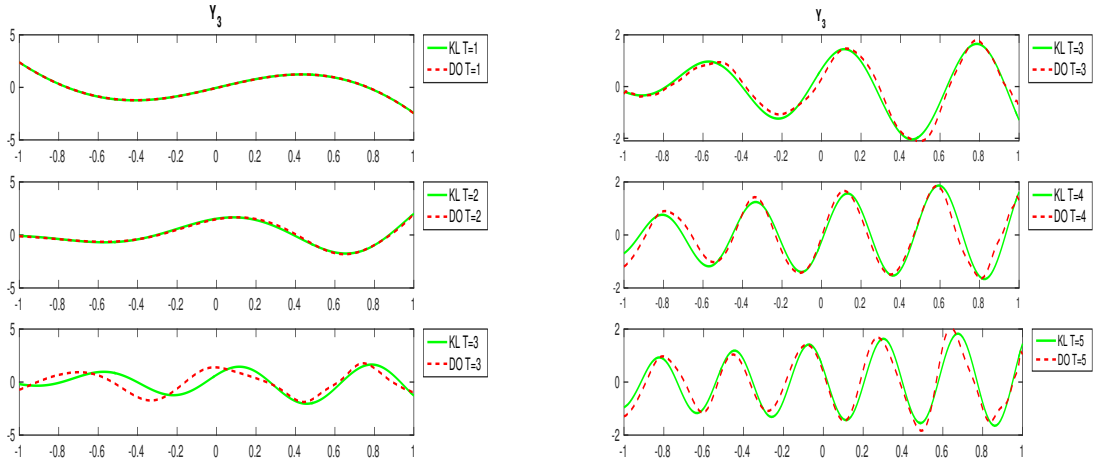

Figure 3: Left: The third stochastic mode of the (constrained) KL decomposition (green) of the reference solution and of the Dual DO approximate solution (red dashed line) with $S = 5$ at time $T = 1$, $T = 2$, $T = 3$ seconds (left) and $S = 11$ at time $T = 3$, $T = 4$, $T = 5$ (right). seconds

random modes of the best rank S approximation at different times. We recall that we denote by $\mathbf{u}_S^{KL}$ the solution to problem (40), namely the best S rank approximation in $\mathcal{M}_{S,div}^{\mathbf{g}_1(t)}$, the approximation manifold with constraints. As expected the accuracy in the evolution of the random basis depends on the number of modes used to compute the Dual DO approximate solution: the modes stay closer and closer to the optimal ones (and for longer time interval) as S increases. In the first part of the transition phase the stochastic modes properly adapt in time also when very few modes are used, whereas the effectiveness of the method tends to decrease for long time intervals, see Figure 2 (right) and Figure 3 (left). Better agreement for longer times is achieved by increasing the number of modes, Figure 3 (right). Similar conclusions can be drawn by analyzing the deterministic modes, see Figure 4 and Figure 5.

We conclude this section by analyzing the rate of convergence of the Dual DO method with respect to the number of modes. The Dual DO approximation error is again computed in norm $H^1(D)\otimes L^2(\Omega)$ with respect to the reference solution computed by using the Stochastic Collocation method and with the same discretization parameters in time and space. In Figure 6 and Figure 7 we compare the Dual DO approximation error to the best approximation error as S increases and at different times. First of all we observe that the approximation error increases in time, due to the intrinsic nature of the exact solution whose rank quickly increases until reaching a stable level when the vortex shedding is fully developed. In particular during the initial phase, for a fixed number of modes, both the DO and the Karhunen-Loève approximation error increase in time, which means that an increasing number of modes are needed to achieve a certain level of accuracy. We observe, however, in Figure 6 that the Dual DO approximation error stays very close the best approximation error and exhibits the same rate of convergence with respect to the number S of modes, until $T \approx 2.4$. On the other hand, Figure 7 shows that the difference between the Dual DO and the best approximation error tends to increase in time when the solution finally reaches the periodic phase. At this stage we observe that the best approximation error stabilizes in time (or slightly decreases). On the other hand, the error of the Dual DO approximation is considerably larger and the convergence rate with respect to S seems to be worse than the one of the best approximation. This result is consistent with the quasi optimal error estimate derived in [32] for linear parabolic problems in which the proportionality constant increases in time.

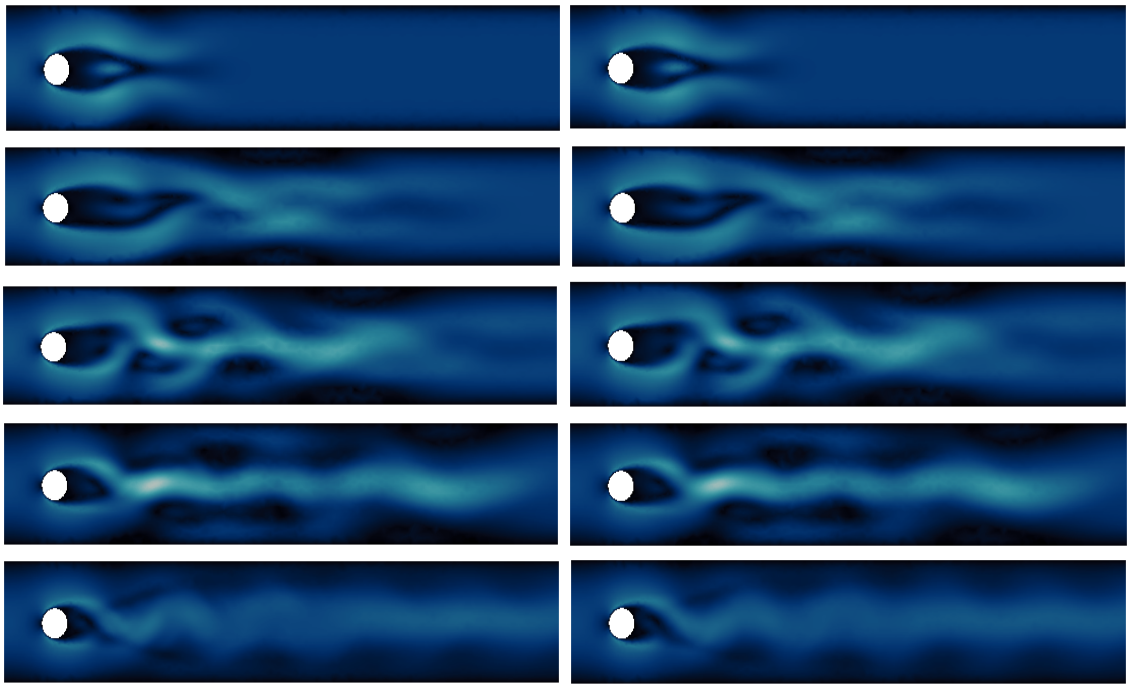

Figure 4: The first deterministic mode of the Dual DO approximate solution with $S = 11$ (on the left) and the first KL eigen-mode of the reference solution (on the right) at $t = 0.6$, $t = 1.6$, $t = 2$, $t = 2.4$ and $t = 5.2$.

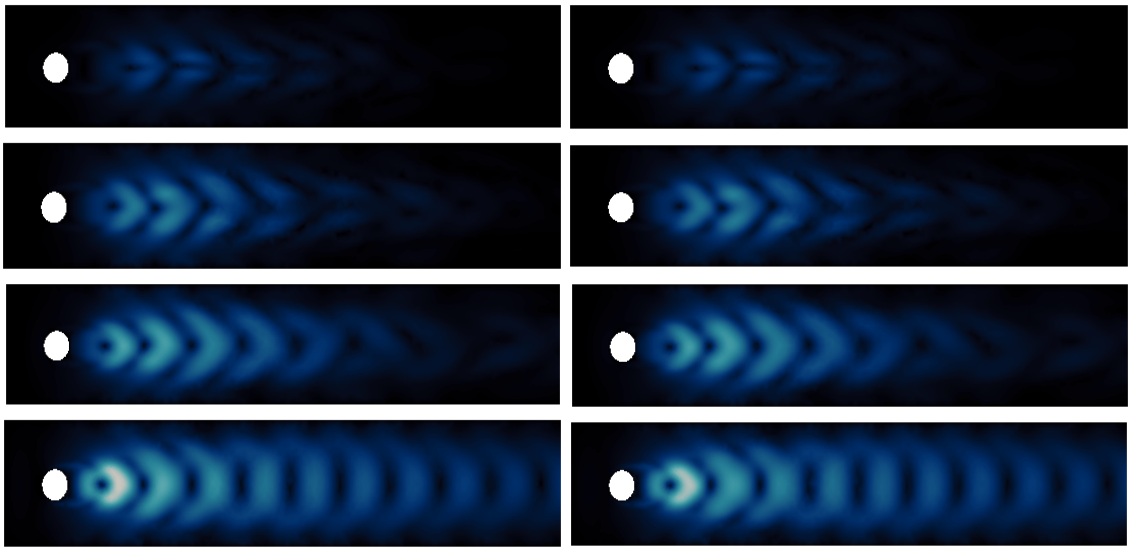

Figure 5: The second deterministic mode of the Dual DO approximate solution with $S = 11$ (on the left) and the second KL eigen-mode of the reference solution (on the right) at $t = 0.6$, $t = 1.6$, $t = 2$, $t = 2.4$ and $t = 5.2$.

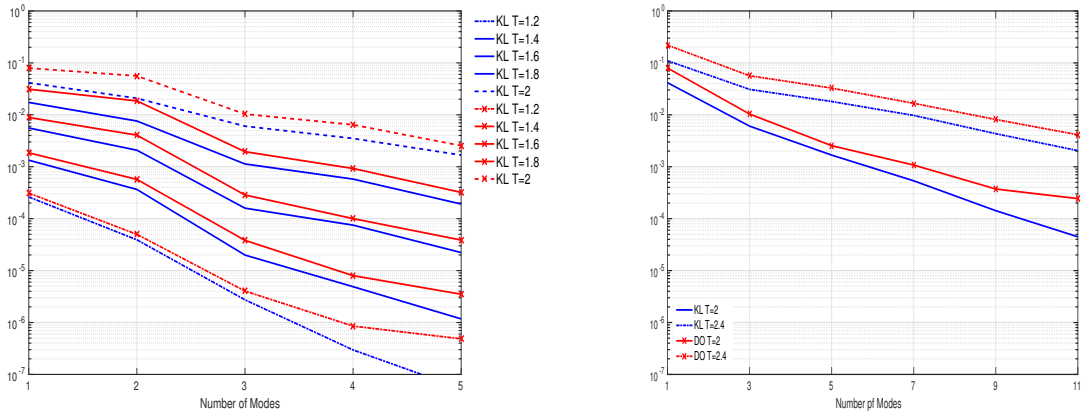

Figure 6: The Dual DO approximation error (red) and the KL truncation error (blue) in norm $H^1(D) \otimes L^2(\Omega)$ with respect to the number of modes, at different time steps (transition phase).

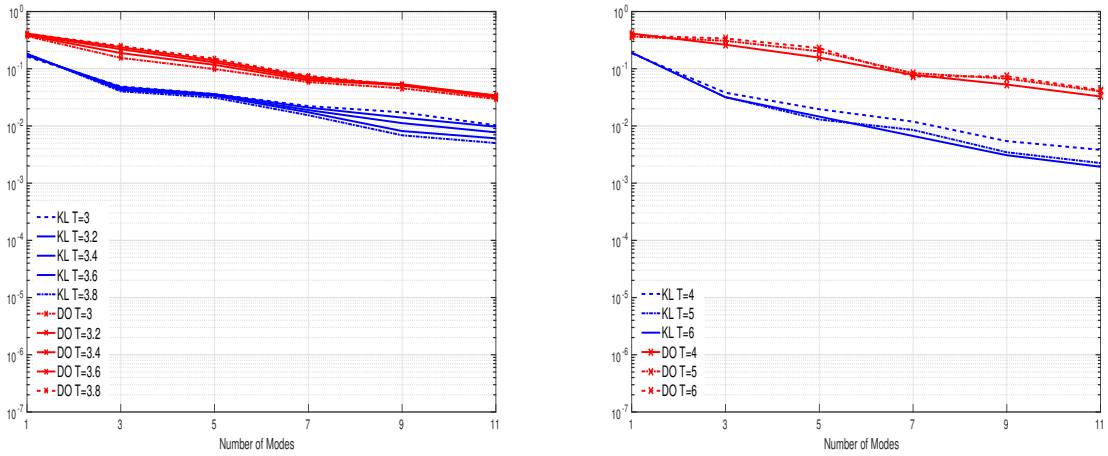

Figure 7: The Dual DO approximation error (red) and the KL truncation error (blue) in norm $H^1(D) \otimes L^2(\Omega)$ with respect to the number of modes, at different time steps (from transition to periodic phase).

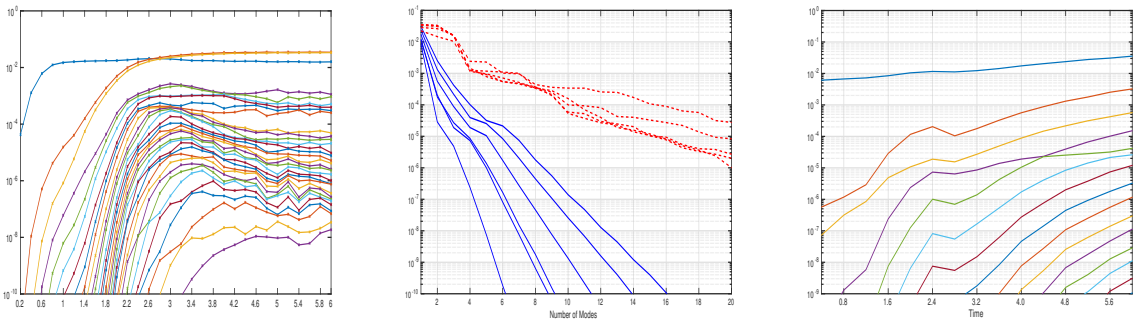

Figure 8: Left: the time evolution of the eigenvalues of u^{KL}, i.e. the Karhunen-Loève decomposition of the reference solution, computed with the stochastic collocation method in a set of $N_y = 33$ Gauss Legendre collocation points. Middle: Decay of the eigenvalues of the Karhunen-Loève decomposition of the reference solution without (red dashed line) and with (blue solid line) time rescaling at different times. Right: the time evolution of the eigenvalues of u^{KL}, i.e. the Karhunen-Loève decomposition of the reference solution with time rescaling.

5.1.2 Time rescaling

The poor performance of the Dual DO method, as any other reduced order method, in efficiently approximate the problem in Section 5.1 for long times, is justified by the intrinsic nature of the solution whose structure is not apt to be well approximated in low rank format. This can be verified by looking at the evolution of the eigenvalues of the covariance operator in Figure 8 (Left): the eigenvalues increase fast and many of them reach not negligible values. Figure 7 shows the rate of convergence for the Karhunen-Loève approximation, i.e. the best approximation with respect to the number of modes in norm $L^2(D) \otimes L^2(\Omega)$. We observe that the decay of the singular values is relatively slow. Moreover we see that the decay significantly changes in time, meaning that the problem is not apt to be approximated by low rank methods with fixed rank. To overcome these problems we propose here a strategy aiming at reformulating the original problem in a new coordinate system in order to obtain a solution that can be suitably approximated in low-rank format. First of all we recall that, for deterministic values of the input parameter, namely for a fixed value of the Reynold's number, the flow features a periodic vortex shedding. In this case POD procedures from snapshots properly collected at different time instants, leads to accurate reconstructions of the solution with few modes. However, as numerically shown e.g. in [33] [28], the accuracy of these methods rapidly deteriorates as one slightly moves away from the parametric value used for the construction of the basis. This is because the input parameters affect the frequency and the length of the recirculation region. In particular when the boundary conditions at the inflow are modeled as in (54), the solutions are velocity fields with varying vortex shedding frequencies which become more and more "out of phase" as time evolves (this explains the increasing rank of the solution in time). In light of that, our goal is to find a transformation which realigns all the solutions and keeps the rank small. For this purpose, we make use of an empirical formula [44] that linearly relates the vortex shedding frequency to the maximum velocity at the inflow: $f_s \propto \frac{U_{max}}{D}$ (where D here is the diameter of the cylinder). We recall that for the problem under consideration $U_{max} = U_m + \sigma z(\omega)$ so we claim that the frequency is linear in the random parameter z. Then, let us consider the fluid motion from a Lagrangian point of view. We define $X(x, s; t)$ the trajectory of the particle that at the instant $t = s$ passes through the point x, and we denote by $\tau = t - s$ the interval of time that the same particle needs to go from x to $x_1 = X(x, s; t)$. We recall that the Navier Stokes equations can be written in Lagrangian form as:

$$\begin{cases} \frac{D\mathbf{u}}{Dt} - \nu\Delta\mathbf{u} + \nabla p = \mathbf{f} \\ \nabla \cdot \mathbf{u} = 0 \end{cases} \tag{59}$$

Observe, however, that in our case the motion is a random field. This implies that, depending on the realization ω, the same particle will need a random interval of time to go from x to x_1. Because of that we define $X(x, s; \tau(\omega))$ the trajectory of the particle that for the realization ω was in x at time s. Observe that now the time is function of the random variable as also the period of the vortex shedding, defined $T = \frac{1}{f_s}$. Our purpose is to find an explicit formula relating T to ω and recover the Eulerian formulation of the motion expressed in terms of the new (random) time variable τ, with respect to which, the period of motion is almost deterministic. By using the empirical formula $f_s \propto \frac{U_m + \sigma z(\omega)}{D}$, we define the new time variable as:

$$(t, \omega) \to \tau(t, \omega) := \frac{U_m + \sigma z(\omega)}{U_m} t$$

(in the following we denote with $\alpha(\omega) = \frac{U_m + \sigma z(\omega)}{U_m}$) and we denote with $\hat{\mathbf{u}}$ the velocity field as a function of τ (instead of t):

$$\begin{cases} \hat{\mathbf{u}}(x, \tau(t, \omega)) = \frac{\partial X}{\partial \tau}(x, s; \tau(t, \omega)) \\ X(x, s; \tau(s, \omega)) = x(\omega) \end{cases}$$

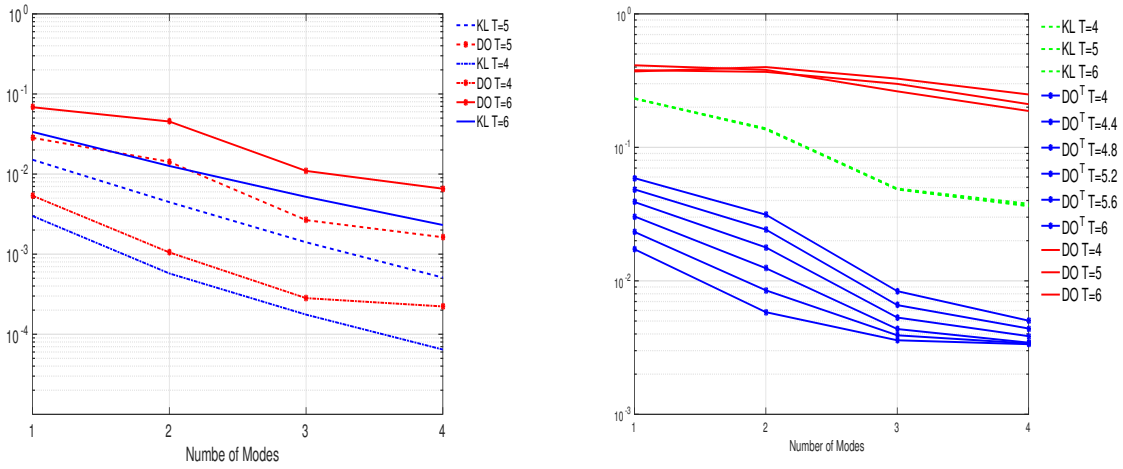

Figure 9: Left: $H^1(D) \otimes L^2(\Omega)$ approximation error with time rescaling. The Dual DO approximation error (red) is compared to the best approximation error (blue) as the number of modes increases and at different time steps. Right: the Dual DO approximation error without (red) and with rescaling (blue, denoted by DO^T) and the best approximation error, all computed in norm $H^1(D) \otimes L^2(\Omega)$ and w.r.t. the reference solution in the original coordinates.

Observe that $\hat{\mathbf{u}} = \frac{1}{\alpha(\omega)} \frac{\partial X}{\partial t} = \frac{1}{\alpha(\omega)} \mathbf{u}$. Then we can rewrite the first equation in (59) with respect to $\hat{\mathbf{u}}$ and τ and we obtain:

$$\alpha^2 \frac{D\hat{\mathbf{u}}}{D\tau} - \alpha\nu\Delta\hat{\mathbf{u}} + \nabla p = \mathbf{f}$$

or equivalently

$$\frac{\partial \hat{\mathbf{u}}}{\partial \tau} + \hat{\mathbf{u}} \cdot \nabla \hat{\mathbf{u}} - \frac{1}{\alpha}\nu\Delta\hat{\mathbf{u}} + \nabla \hat{p} = \hat{\mathbf{f}}$$

In conclusion the problem becomes:

$$\begin{cases} \frac{\partial \hat{\mathbf{u}}}{\partial \tau} + \hat{\mathbf{u}} \cdot \nabla \hat{\mathbf{u}} - \frac{1}{\alpha}\nu\Delta\hat{\mathbf{u}} + \nabla \hat{p} = \mathbf{0} \\ \nabla \cdot \hat{\mathbf{u}} = 0 \end{cases} \tag{60}$$

with deterministic boundary conditions at the inflow:

$$\hat{\mathbf{u}}(\mathbf{x}, \omega, \tau) = (4\bar{U}x_2(H - x_2)/H^2, 0) \quad \mathbf{x} = (x_1, x_2) \in \Gamma_{in}$$

Observe that now the diffusion coefficient is a random variable. We now apply the Dual DO method to problem (60) and we recover the approximate solution of the original problem as $\mathbf{u}_S(\mathbf{x}, \omega, t) = \alpha(\omega)\hat{\mathbf{u}}_S(\mathbf{x}, \omega, \tau(t, \omega))$. The advantage is that $\hat{\mathbf{u}}$ can be more easily approximated in low rank format. Indeed the rate of decay of the singular values of $\hat{\mathbf{u}}$ is significantly faster that the one of $\mathbf{u}$, see Figure 8 (Middle). Figure 8 (Right) shows instead the time evolution of the eigenvalues of the covariance function of $\hat{\mathbf{u}}$. In Figure 9 (Left), the Dual DO approximation is compared to the optimal one. The error is computed in $H^1(D) \otimes L^2(\Omega)$ norm for $\hat{\mathbf{u}}$, so before recovering the approximate solution in the original coordinates. We see that good levels of accuracy can be achieved with very few modes.

We conclude by analyzing the accuracy of the time rescaling technique, once the approximate solution $\mathbf{u}_S = \alpha\hat{\mathbf{u}}_S$ in the original coordinates is recovered. The performances of the time rescaled Dual DO are compared to the Dual DO method applied directly to the original problem (Section 6.2). In Figure 9 (Right) we compare the approximation error of the two approaches: Dual DO approximation without or with time rescaling. Both

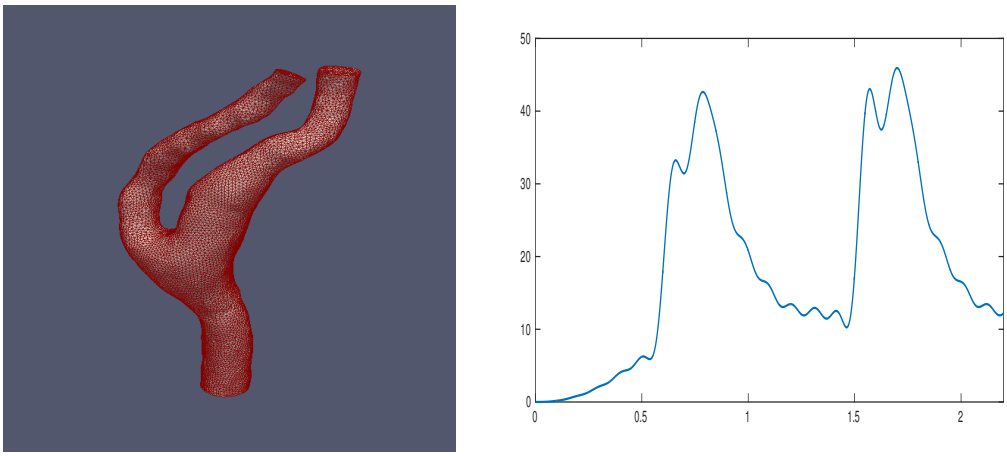

Figure 10: Left: Computational mesh of the carotid artery, having 171123 cells and 34246 vertices. Right: The flow rate at the center of the inflow surface. The data correspond to two heart beats, with an initial quadratic ramp to go smoothly from zero flow rate to the physiological one.

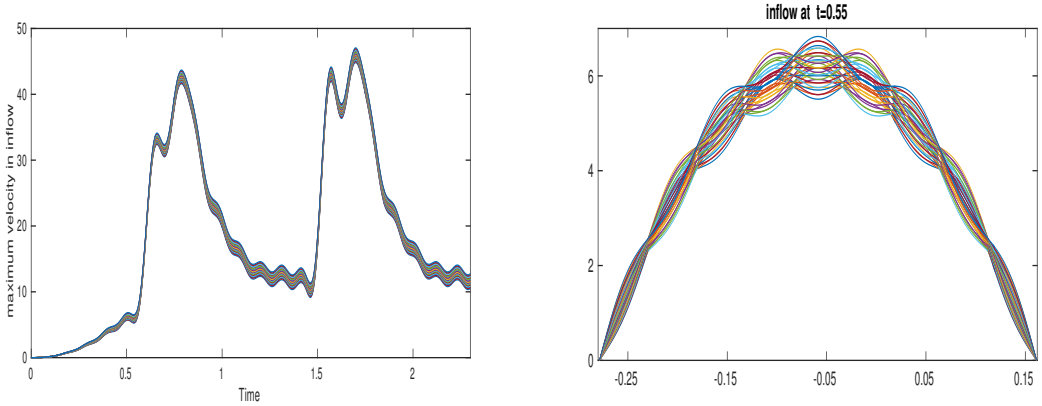

Figure 11: Left: Time evolution of the maximum flow rate in the stochastic collocation points. It corresponds to two heart beat (plus an initial smoothing to agree with the uniform initial condition). Right: Inlet profile in the stochastic collocation points.

the approximate solutions are compared to the reference solution in the original coordinates and the error is computed in $H^1(D) \otimes L^2(\Omega)$ norm. We see that remarkable advantages are obtained by the second approach. Good levels of accuracy can be obtained with very few modes and the error appears to be also smaller than the optimal approximation error of $\mathbf{u}$ (solution without time rescaling) with the same number of modes. However we remark that the error tends to increases for long time, probably due to the fact that we use an empirical formula to approximate the frequency of the solution, quantity that also is very sensitive to computational errors. However this problem seems to be overcome by increasing the number of modes. For the example under consideration, 5 modes are enough to achieve very good levels of accuracy which remains approximately constant in time for the whole computational time interval.

5.2 Hemodynamic application

We now consider the Dual DO method for a hemodynamic problem with real data. Here the Dual DO method has been applied to simulate the blood flow in a realistic carotid artery reconstructed from MRI data

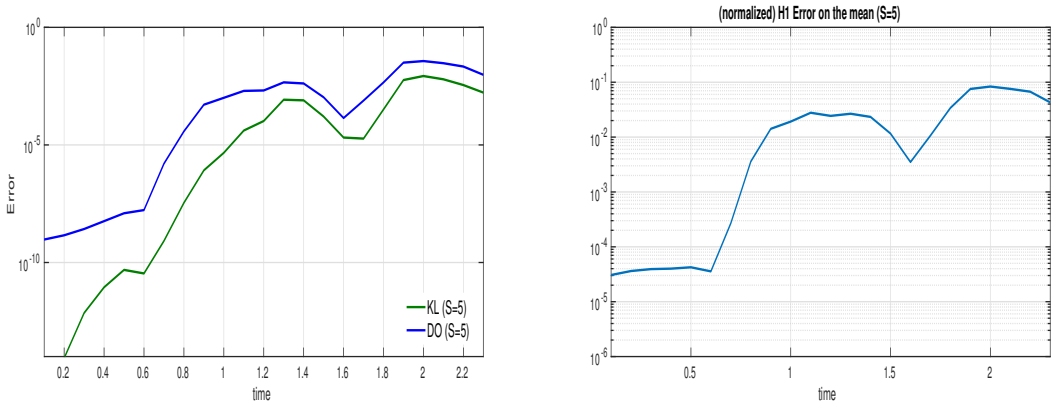

Figure 12: Left: Dual DO approximation error (blue) compared to the best approximation error under boundary constraints. The error is computed in norm $[H^1(D)]^3 \otimes L^2(\Omega)$ with a number of modes $S = 5$. Right: Dual DO approximation error of the mean in norm $[H^1(D)]^3$ with a number of modes $S = 5$.

(MRI images from the *Vascular-surgery and Radiology Divisions at Fondazione IRCSS Ca' Granda, Ospedale Maggiore Policlinico, Milan*): in Figure 10 (left) the mesh used in the numerical simulation, having 171123 cells and 34246 vertices; Figure 10 (right) shows the physiological pulse wave velocity imposed at the inlet, which corresponds to two heart beats. We apply a non-homogeneous Dirichlet boundary condition at the inflow, a homogeneous Neumann condition at the outflow and non-slip conditions at the arterial walls. We assumed random inflow conditions due to possible errors in the Doppler measurements of the axial blood velocity at the inflow section. Specifically at the inlet we consider a parabolic velocity profile perturbed by two uniform and independent random variables Z_1 and Z_2 in $[-1, 1]$ that vary the maximum flow rate and slightly the shape:

$$\mathbf{u}_{|\Gamma_{in}}(\mathbf{x}, t, \omega) = \Big(0, 0, (f_b(t)+Z_1(\omega))(1-(\frac{x^1 - x_c^1}{R})^2-(\frac{x^2 - x_c^2}{R})^2)+Z_2(\omega)\cos(\frac{9(x^1 - x_c^1)}{2R}\pi)\cos(\frac{9(x^2 - x_c^2)}{2R})\Big) \tag{61}$$

(x_c^1, x_c^2) are the coordinates of the center of the inflow section, R is the radius and f_b is the flow rate in figure 10 (right). In Figure 11, the maximum flow rate (left) and the inlet profile (right) for different values of Z_1 and Z_2 is shown. We refer to [4, 34] for the details about the typical numerical and physiological parameters.
We consider the Dual DO formulation with the isolation of the mean describe in Section 4. Let us write the boundary conditions at the inflow as:

$$\begin{aligned} \mathbf{u}(\mathbf{x}, t, \omega) &= \bar{\mathbf{g}}(\mathbf{x}, t) + \mathbf{g}_2(\mathbf{x}, t, \omega) \qquad \mathbf{x} \in \Gamma_{in} \\ \mathbf{g}_2(\mathbf{x}, t, \omega) &= \Big(0, 0, (Z_1(\omega))(1 - (\tfrac{x^1 - x_c^1}{R})^2 - (\tfrac{x^2 - x_c^2}{R})^2) + Z_2(\omega)\cos(\tfrac{9(x^1 - x_c^1)}{2R}\pi)\cos(\tfrac{9(x^2 - x_c^2)}{2R})\Big) \end{aligned}$$

and let $\boldsymbol{\mathcal{M}}_{S,div}^{\mathbf{g}_2(t)}$ denote the manifold of all the divergence free S rank random fields that satisfy the boundary condition $\mathbf{g}_2(t)$ in Γ_D for a fixed $t \in [0, T]$. Hence the approximate solution is sought in the form:

$$\mathbf{u}_S(\mathbf{x}, t, \omega) = \bar{\mathbf{u}}_S(\mathbf{x}, t) + \underbrace{\sum_{i=1}^{S-2} \mathbf{U}_i(\mathbf{x}, t) Y_i(t, \omega) + \sum_{i=1}^{2} \mathbf{U}_i(\mathbf{x}, t) Z_i(\omega)}_{\mathbf{u}_S^*}$$

where $\mathbf{u}_S^*(\cdot, t, \cdot) = \mathbf{u}_S - \bar{\mathbf{u}}_S$ belongs to $\boldsymbol{\mathcal{M}}_{S,div}^{\mathbf{g}_2(t)}$ and $\bar{\mathbf{u}}_S$ is equal to $\bar{\mathbf{g}}$ on Γ_D. The Dual DO reduced system is as in (55). By using the same discretization technique discussed in Section 5.1.1, at each time step we

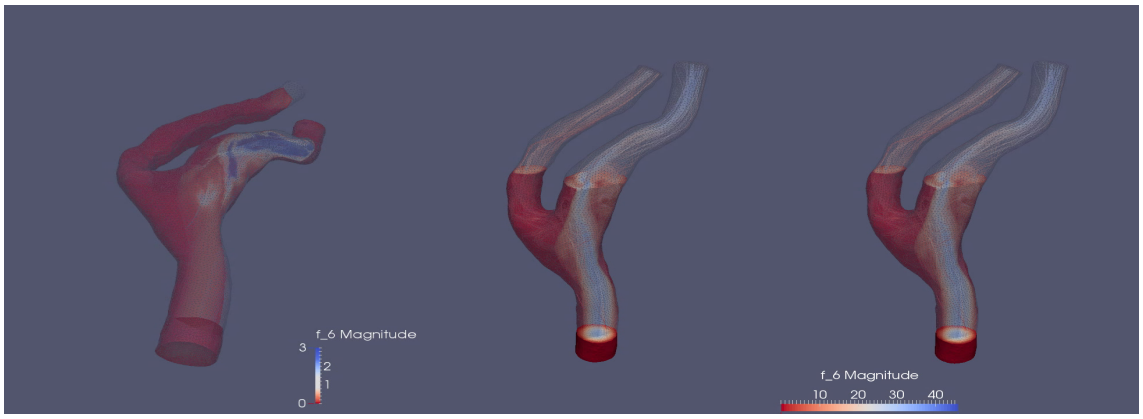

Figure 13: On the left the standard deviation of the solution at time $t = 1.6$ during the second simulated heart beat. On the right we compare the mean of the Dual DO approximate solution computed with 5 modes (right) ($S = 5$) to the mean of the reference solution at the same time. We observe that the approximate solution effectively describes the dynamic and allow to accurately quantify the variability of the solutions.

solve $S + 1$ decoupled deterministic PDEs and $S - 2$ ODEs. We report here the results obtained for $S = 5$. In Figure 12 (left) we compare the Dual DO and the best approximation error in norm $[H^1(D)]^3 \otimes L^2(\Omega)$ as time evolves. We observe that the two errors are proportional and the Dual DO approximate solution stays close to the best S rank approximation. The same conclusions can be drawn by comparing the Dual DO approximation of the mean to the mean of the reference solution, see Figure 12 (right) and Figure 13. Finally in Figure 14,15, 16 we compare the Dual DO modes to the modes of the best approximation. We see that the Dual DO modes adapt properly to describe the variability of the solution. In conclusion for this case the Dual DO method leads to very good results, in term of accuracy versus computational cost.

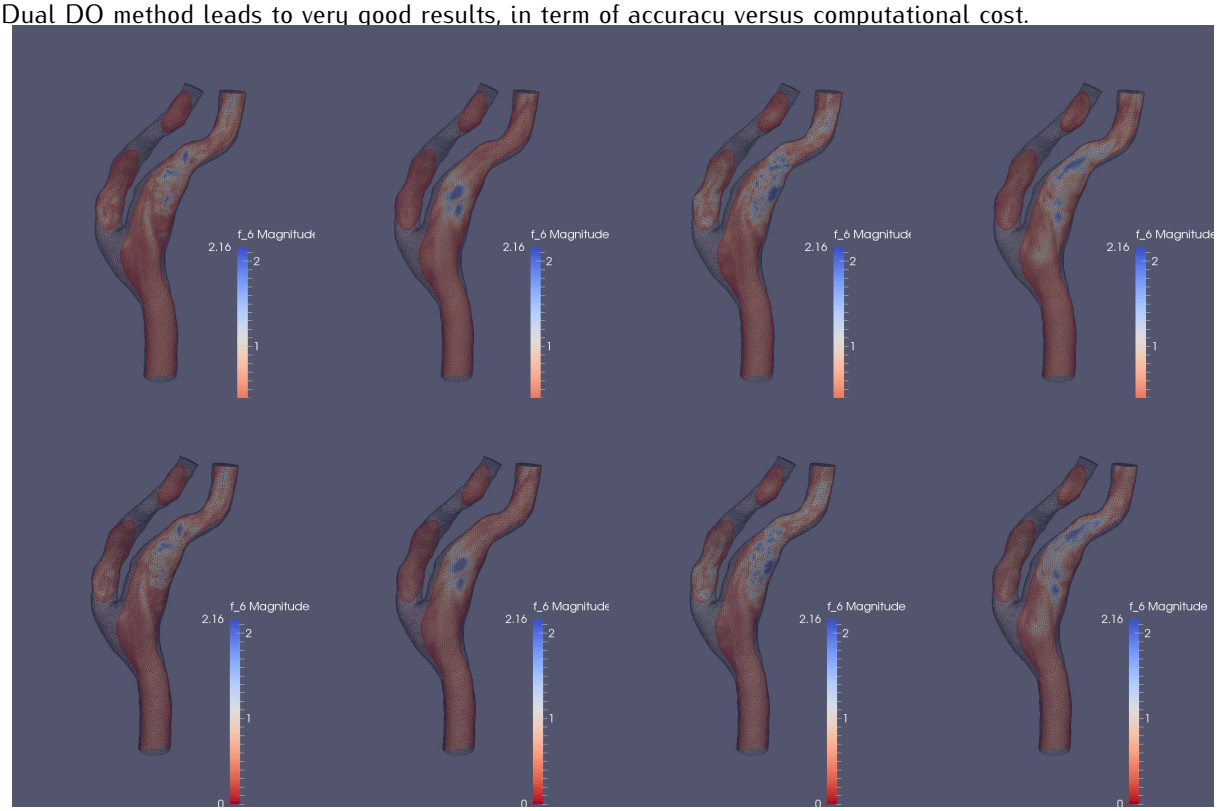

Figure 14: The first deterministic mode of the Dual DO approximate solution with $S = 5$ (on the top) compared and the first eigen-mode of the best approximate solution (on the bottom) at different time

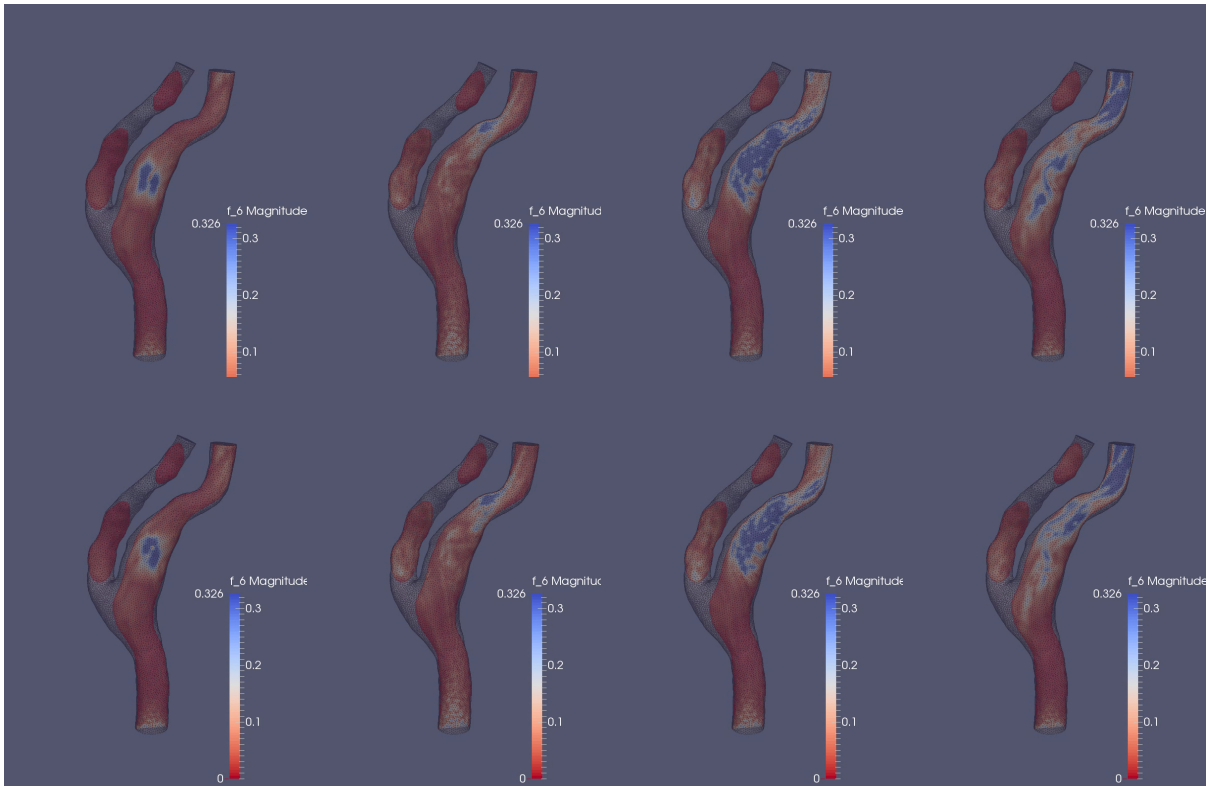

Figure 15: The second deterministic mode of the Dual DO approximate solution with $S = 5$ (on the top) compared and the first eigen-mode of the best approximate solution (on the bottom) at different time

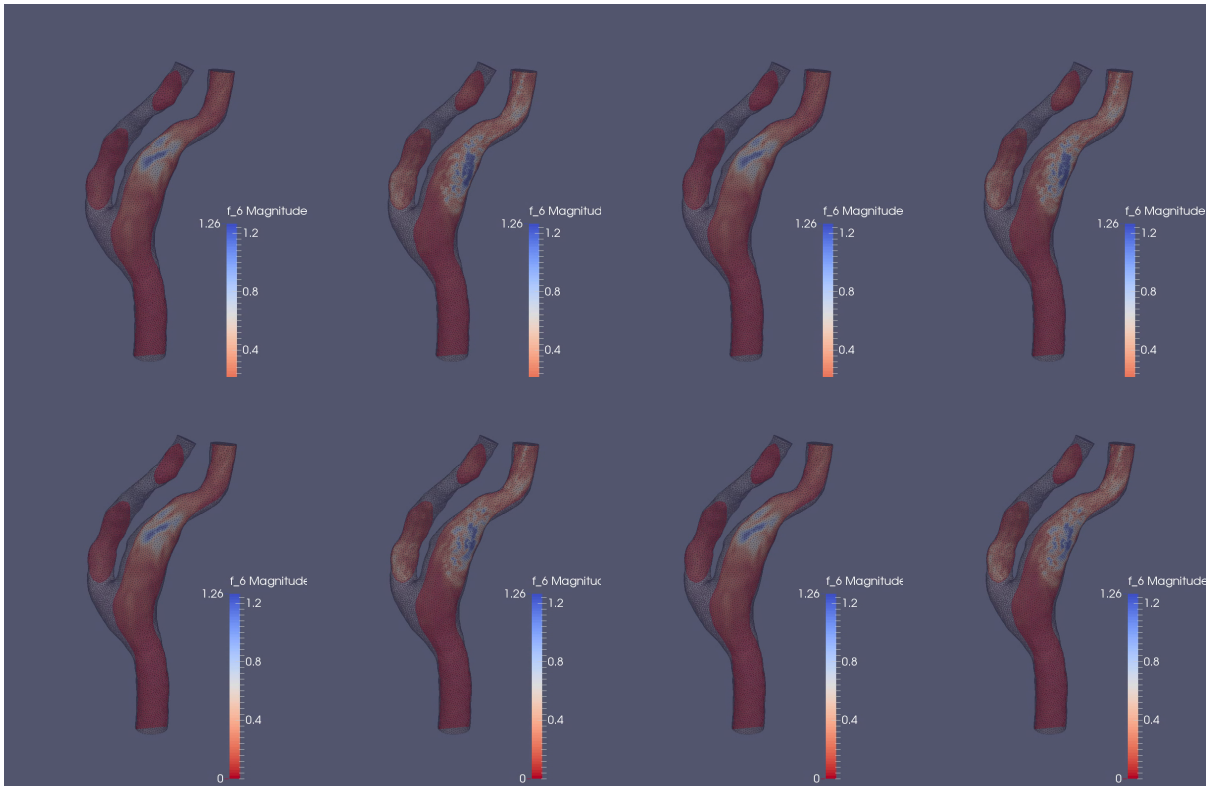

Figure 16: The third deterministic mode of the Dual DO approximate solution with $S = 5$ (on the top) compared and the first eigen-mode of the best approximate solution (on the bottom) at different time

6 Conclusion

In this work we have proposed a convenient strategy to strongly impose random Dirichlet boundary conditions in the dynamically low rank approximation of parabolic PDEs with random parameters. We showed that the set of S rank random fields, constrained to satisfy an approximation of the boundary datum of the exact solution, can be equipped with a structure of differential manifold, allowing for a parametrization of its tangent space in terms of dynamical constraints on the stochastic coefficients. To do so we proposed a Dual DO formulation in which the stochastic modes are kept orthonormal. Under the assumption that the boundary datum g can be properly approximated by a linear combination g_M of $M < S$ terms written in separable form, we fixed M stochastic modes in the approximate solution equal to those in the decomposition of g_M. This allowed us to identify the proper boundary conditions for each (time dependent) deterministic mode and guarantees that the boundary constraint is fulfilled at each time. We obtained a reduced system which consists of a set of S coupled PDEs for the evolution of the deterministic modes, M of which with non homogeneous boundary conditions, coupled with $S - M$ ODEs for the evolution of the stochastic modes. This resulted in an efficient dynamical low rank approximation which accurately takes into account the randomness arising from the boundary data at the price of a slightly reduced flexibility in the evolution of the random modes. Furthermore, we observed that Dual DO formulation is also very convenient to include the incompressibility constraint, when dealing with incompressible Navier Stokes equations. Indeed we were able to effortlessly imposed the solenoidal constraint in each deterministic mode, facilitated by the fact that in the Dual DO formulation no numerical orthonormalization or dynamic constraint is required in the deterministic modes. In conclusion Navier Stokes equations with random parameters, including random Dirichlet boundary conditions, has been reduced to S coupled deterministic PDEs of Navier Stokes type and a system of $S - M$ stochastic ODEs.

We tested the potential and limitations of the proposed method on the classical benchmark 2D problem of an incompressible viscous fluid flowing around a cylindrical obstacle in a channel at moderate Reynold numbers Re$\in [80, 120]$, by adding some randomness in the inflow velocity. The numerical results obtained show good performance of the method, at least at the initial phase, but a loss of accuracy for long time integration. We observed that this is intrinsically due to the fact that the flow patterns become more and more out of phase one with respect to the others, as time evolves, requiring an increasing rank in time to keep a prescribed accuracy level. We numerically showed that a simple time rescaling based on an empirical linear relation between Reynolds number and shedding frequency considerably improves the performance of the method and allows to "rephase" all solutions. Finally we highlighted the potentiality of the Dual DO method for biomedical applications, by simulating blood flows in a realistic carotid artery reconstructed from MRI data, with random inflow boundary conditions. The numerical results reported here, show that good level of accuracy can be achieved with only few modes.

References

[1] C. Bardos, I. Catto, N. Mauser, and S. Trabelsi. Setting and analysis of the multi-configuration time-dependent Hartree–Fock equations. *Archive for Rational Mechanics and Analysis*, 198(1):273–330, 2010.

[2] M. H. Beck, A. Jäckle, G.A. Worth, and H-D. Meyer. The multiconfiguration time-dependent Hartree (MCTDH) method: a highly efficient algorithm for propagating wavepackets. *Physics reports*, 324(1):1–105, 2000.

[3] G. Berkooz, P. Holmes, and J. L. Lumley. The proper orthogonal decomposition in the analysis of turbulent flows. *Annual review of fluid mechanics*, 25(1):539–575, 1993.

[4] R. Botnar, G. Rappitsch, M. B. Scheidegger, D. Liepsch, K. Perktold, and P. Boesiger. Hemodynamics in the carotid artery bifurcation:: a comparison between numerical simulations and in vitro MRI measurements. *Journal of Biomechanics*, 33(2):137 – 144, 2000.

[5] K. Carlberg and C. Farhat. A low-cost, goal-oriented compact proper orthogonal decomposition basis for model reduction of static systems. *International Journal for Numerical Methods in Engineering*, 86(3):381–402, 2011.

[6] M. Cheng, T. Y. Hou, and Z. Zhang. A dynamically bi-orthogonal method for time-dependent stochastic partial differential equations II: Adaptivity and generalizations. *J. Comput. Phys.*, 242:753–776, June 2013.

[7] M. Cheng, T.Y. Hou, and Z. Zhang. A dynamically bi-orthogonal method for time-dependent stochastic partial differential equations I: Derivation and algorithms. *Journal of Computational Physics*, 242:843 – 868, 2013.

[8] F. Chinesta, P. Ladeveze, and E. Cueto. A short review on model order reduction based on proper generalized decomposition. *Archives of Computational Methods in Engineering*, 18:395–404, 2011.

[9] M. Choi, T.P. Sapsis, and G.E. Karniadakis. On the equivalence of dynamically orthogonal and bi-orthogonal methods: Theory and numerical simulations. *Journal of Computational Physics*, 270:1 – 20, 2014.

[10] M. Choi, T.P. Sapsis, and G.E. Karniadakis. A robust bi-orthogonal/dynamically-orthogonal method using the covariance pseudo-inverse for the stochastic Navier-Stokes equations. *preprint*, 2016.

[11] D. Conte and C. Lubich. An error analysis of the multi-configuration time-dependent Hartree method of quantum dynamics. *Mathematical modelling and numerical analysis*, 44(4):759–780, 6 2010.

[12] L. Dieci and T. Eirola. On smooth decompositions of matrices. *SIAM Journal on Matrix Analysis and Applications*, 20(3):800–819, 1999.

[13] R.G. Ghanem and P.D. Spanos. *Stochastic Finite Elements: a Spectral Approach*. Springer–Verlag, New York, 1991.

[14] Robert W Gill. Measurement of blood flow by ultrasound: accuracy and sources of error. *Ultrasound in medicine & biology*, 11(4):625–641, 1985.

[15] J.S. Hesthaven, G. Rozza, and B. Stamm. *Certified reduced basis methods for parametrized partial differential equations*. SpringerBriefs in Mathematics. Springer, Cham; BCAM Basque Center for Applied Mathematics, Bilbao, 2016.

[16] Philip Holmes, John L Lumley, and Gal Berkooz. *Turbulence, coherent structures, dynamical systems and symmetry*. Cambridge university press, 1998.

[17] L. Iapichino. *Reduced basis methods for the solution of parametrized PDEs in repetitive and complex networks with application to CFD*. PhD thesis, École Polytechnique Fédérale de Lausanne, 2012.

[18] O. Koch, W. Kreuzer, and A. Scrinzi. Approximation of the time-dependent electronic Schrödinger equation by MCTDHF. *Appl. Math. Comput.*, 173(2):960–976, February 2006.

[19] O. Koch and C. Lubich. Dynamical low-rank approximation. *SIAM J. Matrix Anal. Appl.*, 29(2):434–454, 2007.

[20] O. Koch and C. Lubich. Regularity of the multi-configuration time-dependent Hartree approximation in quantum molecular dynamics. *ESAIM: Mathematical Modelling and Numerical Analysis*, 41(2):315–331, 2007.

[21] O. Koch and C. Lubich. Dynamical tensor approximation. *SIAM J. Matrix Anal. Appl.*, 31(5):2360–2375, 2010.

[22] O. P. Le Maître and O. M. Knio. *Spectral methods for uncertainty quantification*. Scientific Computation. Springer, New York, 2010. With applications to computational fluid dynamics.

[23] M. Loève. Probability theory, vol. ii. *Graduate texts in mathematics*, 46:0–387, 1978.

[24] G.J. Lord, C.E. Powell, and T. Shardlow. *An introduction to computational stochastic PDEs*. Cambridge Texts in Applied Mathematics. Cambridge University Press, New York, 2014.

[25] C. Lubich. *From quantum to classical molecular dynamics: reduced models and numerical analysis*. European Mathematical Society, 2008.

[26] C. Lubich and I. V. Oseledets. A projector-splitting integrator for dynamical low-rank approximation. *BIT Numerical Mathematics*, 54(1):171–188, 2014.

[27] C. Lubich, T. Rohwedder, R. Schneider, and B. Vandereycken. Dynamical approximation by hierarchical Tucker and tensor-train tensors. *SIAM Journal on Matrix Analysis and Applications*, 34(2):470–494, 2013.

[28] X. Ma and G. E. Karniadakis. A low-dimensional model for simulating three-dimensional cylinder flow. *Journal of Fluid Mechanics*, 458:181–190, 2002.

[29] N.J. Mauser and S. Trabelsi. L2 analysis of the multi-configuration time-dependent Hartree-Fock equations. *Mathematical Models and Methods in Applied Sciences*, 20(11):2053–2073, 2010.

[30] H-D. Meyer, U. Manthe, and L. S. Cederbaum. The multi-configurational time-dependent Hartree approach. *Chemical Physics Letters*, 165(1):73–78, 1990.

[31] Bamdev Mishra, Gilles Meyer, Silvère Bonnabel, and Rodolphe Sepulchre. Fixed-rank matrix factorizations and Riemannian low-rank optimization. *Computational Statistics*, 29(3-4):591–621, 2014.

[32] E. Musharbash, F. Nobile, and T. Zhou. Error analysis of the Dynamically Orthogonal approximation of time dependent random PDEs. *SIAM Journal on Scientific Computing*, 37(2):A776–A810, 2015.

[33] B. R. Noack, K. Afanasiev, M. Morzynski, G. Tadmor, and F. Thiele. A hierarchy of low-dimensional models for the transient and post-transient cylinder wake. *Journal of Fluid Mechanics*, 497:335–363, 2003.

[34] K. Perktold and G. Rappitsch. Computer simulation of local blood flow and vessel mechanics in a compliant carotid artery bifurcation model. *Journal of Biomechanics*, 28(7):845 – 856, 1995.

[35] A. Quarteroni, A. Manzoni, and F. Negri. *Reduced basis methods for partial differential equations*, volume 92 of *Unitext*. Springer, Cham, 2016. An introduction, La Matematica per il 3+2.

[36] Alfio Quarteroni, Alessandro Veneziani, and Christian Vergara. Geometric multiscale modeling of the cardiovascular system, between theory and practice. *Computer Methods in Applied Mechanics and Engineering*, 302:193–252, 2016.

[37] F Riesz and B. Nagy. Functional analysis dover. *New York*, 1990.

[38] T.P. Sapsis and P.F.J. Lermusiaux. Dynamically Orthogonal field equations for continuous stochastic dynamical systems. *Phys. D*, 238(23-24):2347–2360, 2009.

[39] T.P. Sapsis and P.F.J. Lermusiaux. Dynamical criteria for the evolution of the stochastic dimensionality in flows with uncertainty. *Phys. D*, 241(1):60–76, 2012.

[40] R. C. Smith. *Uncertainty quantification*, volume 12 of *Computational Science & Engineering*. Society for Industrial and Applied Mathematics (SIAM), Philadelphia, PA, 2014. Theory, implementation, and applications.

[41] T. J. Sullivan. *Introduction to uncertainty quantification*, volume 63 of *Texts in Applied Mathematics*. Springer, Cham, 2015.

[42] L.J.P. Timmermans, P.D. Minev, and F.N. Van De Vosse. An approximate projection scheme for incompressible flow using spectral elements. *International journal for numerical methods in fluids*, 22(7):673–688, 1996.

[43] X. Wan and G.E. Karniadakis. Long-term behavior of polynomial chaos in stochastic flow simulations. *Comput. Methods Appl. Mech. Engrg.*, 195(41-43):5582–5596, 2006.

[44] F. M. White. Fluid mechanics. 5th. *Boston: McGraw-Hill Book Company*, 2003.

[45] D. Xiu. *Numerical methods for stochastic computations*. Princeton University Press, Princeton, NJ, 2010. A spectral method approach.

[46] J. Zanghellini, M. Kitzler, C. Fabian, T. Brabec, and A. Scrinzi. An MCTDHF approach to multielectron dynamics in laser fields. *Laser Physics*, 13(8):1064–1068, 2003.

Recent publications:

INSTITUTE of MATHEMATICS
MATHICSE Group

Ecole Polytechnique Fédérale (EPFL)

CH-1015 Lausanne

2017

01.2017 LUCA DEDÈ, HARALD GARCKE, KEI FONG LAM:
A Hele-Shaw-Cahn-Hiliard model for incompressible two-phase flows with different densities

02.2017 ROBERT LUCE, OLIVIER SÈTE:
The index of singular zeros of harmonic mappings of anti-analytic degree one

03.2017 ELEONORA MUSHARBASH, FABIO NOBILE:
Dual Dynamically orthogonal approximation of incompressible Navier Stokes equations with random boundary conditions

*****